



저작자표시-비영리-변경금지 2.0 대한민국

이용자는 아래의 조건을 따르는 경우에 한하여 자유롭게

- 이 저작물을 복제, 배포, 전송, 전시, 공연 및 방송할 수 있습니다.

다음과 같은 조건을 따라야 합니다:



저작자표시. 귀하는 원저작자를 표시하여야 합니다.



비영리. 귀하는 이 저작물을 영리 목적으로 이용할 수 없습니다.



변경금지. 귀하는 이 저작물을 개작, 변형 또는 가공할 수 없습니다.

- 귀하는, 이 저작물의 재이용이나 배포의 경우, 이 저작물에 적용된 이용허락조건을 명확하게 나타내어야 합니다.
- 저작권자로부터 별도의 허가를 받으면 이러한 조건들은 적용되지 않습니다.

저작권법에 따른 이용자의 권리는 위의 내용에 의하여 영향을 받지 않습니다.

이것은 [이용허락규약\(Legal Code\)](#)을 이해하기 쉽게 요약한 것입니다.

[Disclaimer](#)

Master's Thesis
석사 학위논문

A Novel Human Detection Scheme and Occlusion
Reasoning using LIDAR-RADAR Sensor Fusion

Seong Kyung Kwon (권성경 權聖景)

Department of Information and Communication Engineering

정보통신융합전공

DGIST

2017

Master's Thesis
석사 학위논문

A Novel Human Detection Scheme and Occlusion
Reasoning using LIDAR-RADAR Sensor Fusion

Seong Kyung Kwon (권 성 경 權 聖 景)

Department of Information and Communication Engineering

정보통신융합전공

DGIST

2017

A Novel Human Detection Scheme and Occlusion Reasoning using LIDAR-RADAR Sensor Fusion

Advisor: Professor Sang Hyuk Son

Co-Advisor: Doctor Jin-Hee Lee

Co-Advisor: Doctor Jonghun Lee

by

Seong Kyung Kwon

Department of Information and Communication Engineering

DGIST

A thesis submitted to the faculty of DGIST in partial fulfillment of the requirements for the degree of Master of Science in the Department of Information and Communication Engineering. The study was conducted in accordance with Code of Research Ethics¹

10. 6. 2016

Approved by

Professor (Advisor)	Sang Hyuk Son	<u> (Signature)</u>
Doctor (Co-Advisor)	Jin-Hee Lee	<u> (Signature)</u>
Doctor (Co-Advisor)	Jonghun Lee	<u> (Signature)</u>

¹ Declaration of Ethical Conduct in Research: I, as a graduate student of DGIST, hereby declare that I have not committed any acts that may damage the credibility of my research. These include, but are not limited to: falsification, thesis written by someone else, distortion of research findings or plagiarism. I affirm that my thesis contains honest conclusions based on my own careful research under the guidance of my thesis advisor.

A Novel Human Detection Scheme and Occlusion Reasoning using LIDAR-RADAR Sensor Fusion

Seong Kyung Kwon

Accepted in partial fulfillment of the requirements for the degree of Master of Science.

10. 6. 2016

Head of Committee _____(인)

Prof. Sang Hyuk Son

Committee Member _____(인)

Dr. Jin-Hee Lee

Committee Member _____(인)

Dr. Jonghun Lee

MS/IC
201522003

권 성 경. Seong Kyung Kwon. A Novel Pedestrian Detection Scheme and Occlusion Reasoning using LIDAR-RADAR Fusion. Department of Information and Communication Engineering. 2016. 57p. Advisor Prof. Sang Hyuk Son, Co-Advisor Dr. Jin-Hee Lee, Co-Advisor Dr. Jonghun Lee.

ABSTRACT

Human detection technologies are widely used in smart homes and autonomous vehicles. In addition, object detections are critical technologies for the safety of pedestrians and drivers in the autonomous vehicles. However, in order to detect human, autonomous vehicle researchers have used a high-resolution LIDAR and smart home researchers have applied a camera with a narrow detection range. Despite the development of sensors and their sensor fusion technologies in order to improve the accuracy of object detection, occluded pedestrian detection technology remains a still challenging topic. Conventional occluded pedestrian detection has utilized a camera that extracts a variety of characteristics such as their color and contour of objects. However, a camera has vulnerabilities like as high sensitivity of environmental changes and high complexity of image processing. LIDAR-RADAR fusion method has been mainly used to recognize moving vehicles since the method can estimate their velocities by using Doppler Effect. Also, the fusion method is robust about environmental changes and weather conditions. Furthermore, to our best knowledge, the occluded pedestrian detection using LIDAR-RADAR fusion has not yet been reported. These studies for occluded pedestrian detection employ camera-based methods that have characteristics such as much sensitiveness and heavy image processing. To solve these problems, we propose a new occluded depth generation based reasoning method utilizing a LIDAR-RADAR sensor fusion. In order to classify the human, we concomitantly propose a novel method with a low-cost and low-resolution LIDAR that can detect human quickly and precisely without complex learning algorithm and additional devices. In other words, the human can be distinguished from objects by

using a new human characteristics function which is empirically extracted from the characteristics of a human. The proposed method consists of object detection, occluded depth generation, and then occluded pedestrian detection. Occluded depth generation is an effective means to find out an obscured area hidden by any obstacles. The objects within the occluded depth are detected by RADAR and an occluded object is estimated as a pedestrian by means of unique human Doppler distribution measured from RADAR. In addition, the proposed method has low processing computation in comparison with conventional learning methods because it generates precise fusion ROI (Region of Interest) by combining ROIs of each sensor. Therefore, an occluded pedestrian can be estimated by utilizing the RADAR Doppler pattern and the LIDAR human characteristics curve within the fusion ROI. In addition, we verified the effectiveness of the proposed algorithm through a number of experiments.

Keywords: Pedestrian detection; LIDAR-RADAR sensor fusion; Human Characteristic Function; Occluded Object detection; Occluded depth generation

Contents

Abstract	i
List of contents	iii
List of table	iv
List of figures	iv
I. Introduction	1
II. Related Work	5
III. LIDAR-based Human Detection	8
1. Conventional LIDAR-based human detection methods	8
2. Human Characteristic Function	9
3. Experiments	13
4. Conclusion	21
IV. Occluded Pedestrian Detection	22
1. Conventional Occluded Object Detection Systems	22
2. Occluded Depth based Occlusion Reasoning Scheme	23
3. Experiments	30
4. Conclusion	46
V. Summary and Future work	48
References	51
요약문	56

List of tables

TABLE 1. The human characteristics curve of typical human postures	25
TABLE 2. Specification of LIDAR and RADAR	31
TABLE 3. Indoor environments of measurement scenarios	32
TABLE 4. Outdoor environments of measurement scenarios	33
TABLE 5. Detection rate for each scenarios	46

List of figures

Figure 1. Human pattern distribution data extracting from 2D LIDAR	9
Figure 2. The results of the polynomial fitting curve	11
Figure 3. A Human characteristics function fitted to a quadratic curve	13
Figure 4. Comparison results of detection rate according to order selection of a high-order polynomial equation in a human characteristics function	15
Figure 5. Detection rate of single target according to conventional clustering methods	16
Figure 6. Range error between the actual object and the detected object	16
Figure 7. A human pattern from low resolution LIDAR dataset	18
Figure 8. Multi-targets experiment environment	19
Figure 9. Multi-targets detection rate of the proposed algorithm and other clustering methods using pattern recognition	20
Figure 10. The proposed occluded objects detection scheme using LIDAR and RADAR sensor fusion	24
Figure 11. Occluded depth generation process	27
Figure 12. Occluded depth based LIDAR and RADAR scheme	29
Figure 13. The results of scenario (i)	34
Figure 14. The results of scenario (ii)	36

Figure 15. The results of scenario (iii) 40
Figure 16. The results of scenario (iv)41
Figure 17. The results of scenario (v) 42
Figure 18. The results of scenario (vi)45

I. Introduction

Smart Home and autonomous vehicles are research areas that are important applications of IoT (Internet of Things). One of the important topics to deal with this research field is the human detection technology. The human detection technology has been applied to the smart home is used to provide services such as delivery of the products on the basis of the user position [1]. The methods utilizing a variety of sensors have been proposed to determine the location of human in the room. The general methods used for the human detection in the room utilize the camera, the motion sensor, and the ultrasonic sensor. The camera has been applied to the methods such as facial recognition and motion recognition for human detection. However, the camera is sensitive by intensity changes of the light, and it has a narrow detection range as well as privacy issues [2-3]. In addition, multiple cameras or more additional devices are required in order to expand the detection range. Another methods have used ultrasonic sensors or motion sensor. Those require to attach the sensor previously. Also, the methods show a difference performance according to the mounting position of sensors [4-5]. The methods are possible to detect multiple targets and a moving target. However, the methods are difficult to classify whether the detected target is the human or not.

Furthermore, human detection technology has been applied for safety of pedestrian and driver in autonomous vehicle field [6-8]. The various techniques have been applied to develop autonomous driving technologies such as ADAS (Advanced Driver Assistance System), ASCC (Advanced Smart Cruise Control), LKAS (Lane Keeping Assist System), and AEB (Autonomous Emergency Braking system). In spite of the developed technologies, pedestrian accident has been annually increased at a higher rate. According to the US statistics, pedestrian fatalities in traffic crashes are annually more than 10% of the total fatalities from 2004 to 2013. Also, most accidents

have occurred at night [7]. According to the EU statistics, pedestrian fatalities in road traffic crashes are about 22% in 2013 [8].

Technologies for detecting objects such as a pedestrian have been continuously developed to use camera, LIDAR and RADAR. These sensors are utilized on the basis of intrinsic characteristic for object detection. Information of the object such as the color and contour can be obtained by images extracted from camera. Object detection method using a camera is easily accessible, since many studies have been developed in the autonomous vehicle field [6, 9, 10-16]. In addition, peculiarities of the camera are high object detection and an affordable price. However, the sensor has demerits such as high sensitiveness and complex processing computation. LIDAR is able to measure precise distance between the sensor and the object. In addition, the sensor has wide field of view and is robustness on environment change. On the other hand, since the classification based on the shape of the object, LIDAR has low recognition performance compared to the camera. RADAR can extract the distance by means of velocity of object based on Doppler Effect. However, RADAR is difficult to accurately recognize the object and has heavy processing time owing to using the scattered signal.

The development of the sensors and the algorithm for overcoming the vulnerabilities of the sensors has been actively carried out. For example, the camera sensor has been used for the object detection techniques such as Haar-like or HOG (Histogram of Oriented Gradient) [6, 17-18]. In addition, the techniques have applied various machine learning algorithm such as AdaBoost and Support Vector Machine (SVM) in order to classify the object [6, 18-19]. Moreover, sensor fusion techniques has been proposed for the object detection method. LIDAR-camera fusion technique has used the ROI of the object extracted from LIDAR for reducing image processing time of camera

[20]. Conventional LIDAR-RADAR fusion technique is mainly applied to detect the vehicle and the motorcycle [21-22]. The studies have suggested the object detection using Doppler information obtained from RADAR and width and length information of vehicle acquired from LIDAR. However, there are detection constraints for slow moving target with low reflectivity such as pedestrian because these techniques aim to detect fast moving target with high reflectivity. In particular, when the pedestrian is partially obscured by another object, there is a tremendous difficulty to detect the occlude pedestrian [16]. To detect occluded object, there are researches using sensor fusion technique and machine learning algorithm based on a camera [14, 23–27]. The sensor fusion techniques using camera are available for detecting and recognizing the object since they extract the similarity between the object detected from the sensor and the training data applying the machine learning. However, these methods are difficult to process in real time owing to extracting a variety of features and performing the learning process using a camera. Also, these methods using the camera are influenced on the environment change such as light intensity.

In this paper, a human characteristic function using a low-cost LIDAR is proposed to detect human in indoor environment. The proposed method extracts the data pattern of the human that is expressed by higher-order function from the LIDAR. The method utilizes the data extracted from LIDAR data with low resolution. A novel human characteristic function based on the proposed method is used to detect the human in real time without machine learning. In addition, occluded pedestrian detection scheme using LIDAR-RADAR fusion technique is proposed to reduce processing complexity and to ensure the robust detection performance. The proposed method has concept of fusion ROI and occluded volume. The fusion ROI is generated by overlapped area of two ROIs produced by LIDAR and RADAR sensor. The computation time of the algorithm reduces through accurate ROI setting. The concept of occluded volume is introduced in order to estimate

the presence of the target that is obscured by another object, and it is generated from LIDAR. The occluded object cannot be observed by LIDAR, but it is able to measure from RADAR. Therefore, the object inside occluded volume is estimated as occluded pedestrian candidate through reasoning method using RADAR. Finally, the occluded pedestrian is determined by analyzing the Doppler pattern obtained from RADAR.

The rest of this paper is organized as the follows. Section II represents the related works. Section III explains the human characteristic function. A occluded pedestrian detection algorithm is handled in section IV. Finally, section V reports the summarizing remarks.

II. Related Work

Conventional human detection technologies use a variety of sensors such as the camera, the ultrasonic sensor, motion sensor, and the LIDAR. In this section, the previous researches are introduced to use the sensors for object detection.

The camera sensor mainly has been used for the object detection in indoor as well as outdoor environment. The ultrasonic sensors are used to detect the distance data between the sensor and the object. However, the ultrasonic sensors are difficult to classify the object. In addition, the general methods using the ultrasonic sensors are important that the installation place of the sensor because this sensor has a narrow field of view. If the object is detected by the ultrasonic sensor, a complex algorithm is required to classify the object, such as fuzzy logic, fast Fourier transform, and machine learning [28]. Therefore, the method using the ultrasonic sensors has heavy computation to detect the human.

The motion sensors have similar problems with an ultrasonic sensor. The motion sensor detects the human as well as the moving object such as a dog and a mobile robot. Therefore, the sensor to classify the human also requires additional complex algorithms. In addition, the sensor has various results as the human posture and the deployment of other sensors [29]. Therefore, the sensor is hardly suitable for the detection algorithm of the human in outdoor environments.

LIDAR-Camera sensor fusion has been used for object detection generally. Camera is sensitive to changes in brightness of the light and it has complex image processing. LIDAR is difficult to recognize the color and to classify objects in comparison with the camera. Sensor fusion technologies have been applied to overcome the shortcomings of each sensor and to improve the

performance. LIDAR-Camera sensor fusion is usually composed of three steps: calibration, feature extraction, and classification [20].

The first step is a calibration process that is to match the coordinate of the LIDAR and camera. In calibration step, the distance between an object and two sensors is measured, and the position error is corrected. The second step is to extract information of objects using LIDAR data. When using a 2D LIDAR, width and thickness of the object are obtained. Whereas, width, thickness and height of the object are extracted from 3D LIDAR. The final step is the objects classification using a camera. The position of the objects is calculated in previous step. The image obtained from the camera is divided based on the position of object. The classification process is performed to use machine learning such as SVM (Support Vector Machine) and AdaBoost.

LIDAR-RADAR sensor fusion is robust than cameras to environmental change because it uses the signal of the laser and radio frequency [22, 30-35]. Conventional LIDAR-RADAR fusion is most applied to detect the vehicle, and research on detection of pedestrian with partially obscured pedestrian is at an early stage. In previous methods, the vehicle is estimated by using the information of width, length and shape of the object obtained from LIDAR. Then, the velocity of the object is acquired from RADAR [32]. The typical vehicle detection process using LIDAR-RADAR sensor fusion is composed by several steps.

First step is the environment and vehicles perception from LIDAR. In sensor fusion state, LIDAR can be used to the surrounding environment perception, because it has high confidence of distance and angle resolution [22]. In addition, it can be determined whether or not the vehicle through the shape of the objects. Based on this, it generates a road information and vehicle hypothesis, and transmit by RADAR. Next is RADAR measurement. At this point it is possible to

measure the speed of objects through the RADAR applying the Doppler Effect [30]. When the vehicle hypothesis is determined, RADAR is to obtain the speed of the objects. This techniques are applied to the Adaptive Smart Cruise Control (ASCC) in order to follow the preceding vehicle.

III. LIDAR-Based Human Detection

1. Conventional LIDAR-based Human Detection

Human detection methods have been developed to use LIDAR [9, 17-18, 20, 36]. The typical methods using LIDAR are applied for measuring the body ratio [37] and detecting the legs [6]. The body ratio in the methods is estimated by the ratio between width and length of the human. The legs detection method is classified by the distance correlation between the legs of the human. The methods are composed with clustering and classification. The data of the human obtained from LIDAR are represented as the scatter points. The clustering is performed to merge the data based on the distance associativity. After that, the features of the human such as width and length of the body are obtained from the sensor data. The extracted features are utilized to classify the objects in classification step. The classification step mainly uses the machine learning approach [6]. The general learning methods are Bayes classifier, AdaBoost, and SVM (Support Vector Machines). When the preliminary obtained data is large, the Bayes classifier has high accuracy because it is based on a probability model. AdaBoost method is one of the boosting algorithms. The AdaBoost performs classification with the weak classifiers and a change of the weight, repeatedly [6]. SVM is a learning model for the pattern recognition and data analysis, and a kernel is applied [38].

However, the previous methods using LIDAR are difficult to classify the object which has a similar shape with the human. In addition, the methods have heavy processing time by using learning algorithm. To address this problem, a novel human detection method is proposed in this section. The proposed method is performed by based on the body characteristic of the human without using machine learning. The body characteristic of the human is similar to the higher-order polynomial curve. In this section, we provide the fitting method for correcting the data of the human

as a criteria of classification. The proposed method is able to classify the human rapidly since the characteristic of the human is only used.

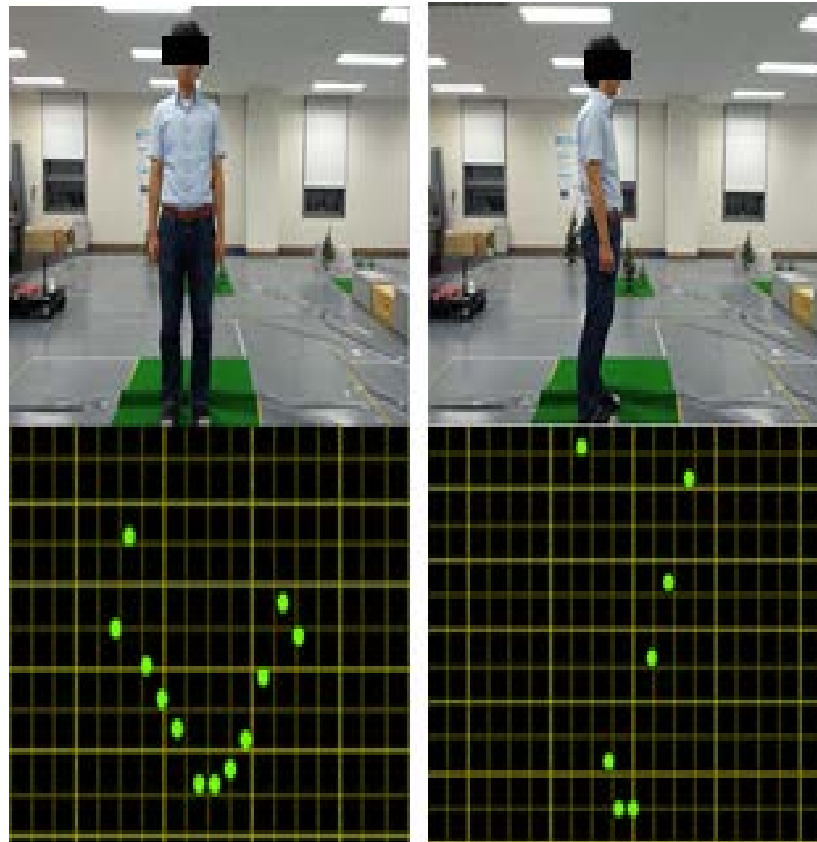


Figure 1. Human pattern distribution data extracting from 2D LIDAR: (a) front position and (b) side position

2. Human Characteristic Function

In this section, the method using low-resolution LIDAR is proposed for human detection without using any learning process. The proposed method extracts the higher-order HCF (Human Characteristics Function) by determining the human, experimentally. In addition, the obtained data is corrected by HCF and is classified to use a slope of HCF based on the characteristic of human as streamline. Figure 1 shows the LIDAR data which are extracted from the front pose and the side

pose of the human. The human body has the features of the higher-order polynomial curve distribution as shown in Figure 1. In addition, the clustering is performed to group the data of the human with the features of the higher-order polynomial curve distribution.

2.1. Clustering

LIDAR has one output per the horizontal angular resolution. Therefore, the LIDAR has a lot of output by continuous scanning all of the horizontal angular resolution in order to detect a single object. The process of grouping a number of points is the clustering. The general clustering methods are distance-based clustering, GMM (Gaussian Mixture Model) clustering, and K-Means clustering. The distance-based clustering is the method to merge the adjacent points closer than threshold value. The distance between the points is calculated by Euclidean distance in Equation 1. x_i and y_i are represented by the coordinate of the i^{th} data.

$$d_i = \sqrt{([x_i] - [x_{i-1}])^2 + ([y_i] - [y_{i-1}])^2} \quad (1)$$

GMM utilizes the combination of Gpdf (Gaussian probability density function), and it is consisted of ML (Maximum Likelihood) and EM (Expectation Maximization) algorithm [6, 39]. GMM calculates the estimated value of the entire training data through the ML. The parameter obtained as a result of the ML requires the estimated values of other parameters. EM algorithm is used to obtain the estimated value. K-Means clustering divides the data into k groups based on the distance in order to minimize the cost function and the dissimilarity [40]. The degree of similarity of the data in the same group increases and the degree of similarity of the data between different groups decreases. The cost function defines the sum of the square of the distance between the center of each group and the data. The initial value of K-means is carefully considered for setting because

its result is significantly influenced by it. In this paper, we use the distance-based clustering to reduce the computation complexity.

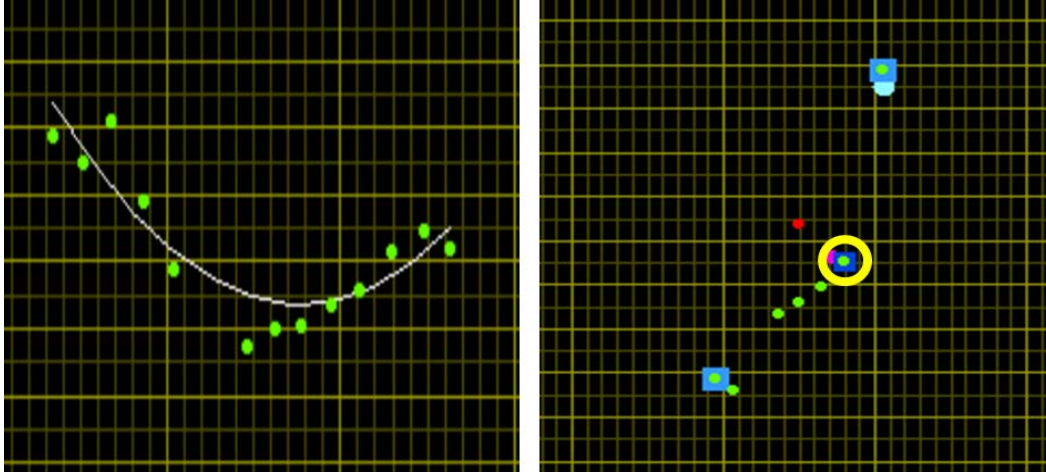


Figure 2. The results of the polynomial fitting curve: (a) The second order polynomial fitting curve based on LIDAR data, (b) middle point of human

2.2. Classification

Classification methods use machine learning such as SVM and AdaBoost. However, the method requires the process to find a variety of features with a plurality of data. On the other hand, a low-resolution LIDAR used in this paper does not have constant output data and lacks of the amount of the data compared to a high resolution LIDAR. If width and length of the objects are only used to classify the human, another objects similar to the width and length of human are detected at the same time. To overcome this problem, the proposed method is performed to correct the non-uniform output data. In addition, the method uses the unique characteristic of human using higher-order polynomial curve in order to classify the human and objects. Therefore, the features of the width, length, and slope of the human are obtained by approximating the non-uniform output data with

higher-order polynomial curve. Figure 2 shows the quadratic curve and the object centroid after approximating the LIDAR output data. The points of the cluster obtained in the previous step are used to present a quadratic polynomial curve. The polynomial equation $f(x_i)$ composed with i^{th} coordinate is defined by Equation 2. x_i^j and a_j represent an input sequence of i^{th} coordinate and the coefficient. In addition, j presents the polynomial order and can has maximum value m . The output array of the LIDAR is expressed by Equation 3, and y_i is i^{th} coordinate.

$$f(x_i) = \sum_{j=0}^m a_j x_i^j \quad (2)$$

$$y_i = \sum_{j=0}^m a_j (x_i)^j \quad (3)$$

$$a_j = \frac{1}{N} \sum_{i=0}^{N-1} w_i (f(x_i) - y_i)^2 \quad (4)$$

The polynomial coefficient a_j in order to minimize the error using the least squares method is provided by Equation 4. N is the length of the output array y_i , and w_i is the weight of the i^{th} element. The quadratic curve has $m=1$ and it is presented as a_0 and a_1 calculated by Equation 4. Then, the output array y_i is estimated whether the human or not.

The high resolution LIDAR is possible to enough obtain the output data for detecting the object. However, the low resolution LIDAR does not have enough data. In this paper, the calibration process is required as shown in Figure 3 and we apply the quadratic curve because the human is detected to use the human characteristic based on insufficient output data. In Figure 3, the width d_x is indicated by the yellow line, and the length d_y is represented by blue line. The green points are the object data extracted from LIDAR, and the red curve is a quadratic curve based on the LIDAR data. The human is classified by using the width, length, and slope of a quadratic curve.

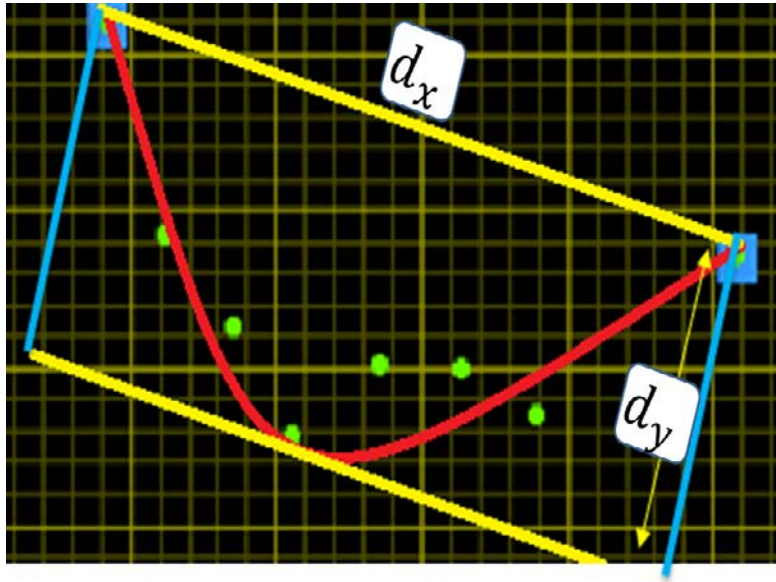


Figure 3. A human characteristics function fitted to a quadratic curve

3. Experiments

In this section, we experimentally verify that the result using the second-order polynomial curve shows the improved results compared to the result of the other higher-order polynomial curve for detecting the human. The experimental environment is configured as a single target and multiple targets. In a single target environment, there is only one person without any obstacles around. Multi-target experimental environment is consisted of three human, three obstacles with a width and thickness similar to the human, and one wall. Through the experiment, the proposed algorithm is verified to detect the human using the low resolution LIDAR.

3.1. Order Selection

The shape of the human is detected to determine the optimal-order of human characteristic function in the single target environment and multi-target environment. Then, the human detection rate is compared by increasing the polynomial degree from the primary polynomial curve to the quartic curve. The data of ten subjects are collected in the equal environment, and those are calculated by the polynomial order, respectively. In addition, the average of the width and the thickness of the subjects are estimated by them.

Figure 4 shows the detection rate of the human measured by each polynomial order in the single and the multiple target environments. A quadratic polynomial curve has the best detection rate 95 % in 3239 frames. The human can be detected by a primary polynomial straight in a single target environment. However, the primary polynomial straight is not possible to distinguish the human and the obstacle in a multi-target environment. The higher-order polynomial curve shows a similar shape of the human as a flexible curve. On the other hand, the higher-order polynomial curve is difficult to classify the target because the flexible curve can express a similar shape of the human and the obstacle. The human characteristic function using the quadratic polynomial curve is verified as the most suitable curve for detecting the shape of the human by applying the LIDAR data, through the experiment.



Figure 4. Comparison results of detection rate according to order selection of a high-order polynomial equation in a human characteristics function

3.2. Feature Extraction

In this paper, a single target experiment is performed to compare the method using the HCF with the other clustering methods. GMMC and K-Means are methods having a decent performance. However, GMMC and K-Means show incorrect result by using the low resolution LIDAR because the output data disappears repeatedly. In addition, these methods take a lot of calculation time in comparison with distance-based clustering. Therefore, the distance-based clustering in this paper is applied for evaluating the HCF.

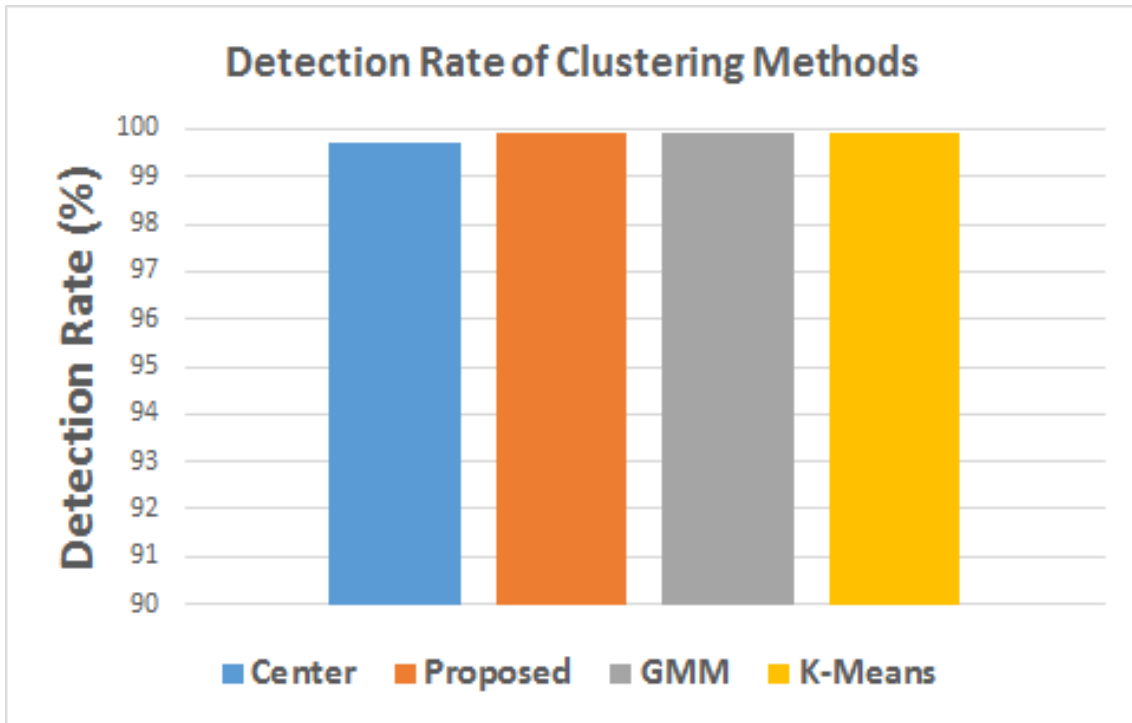


Figure 5. Detection rate of single target according to conventional clustering methods

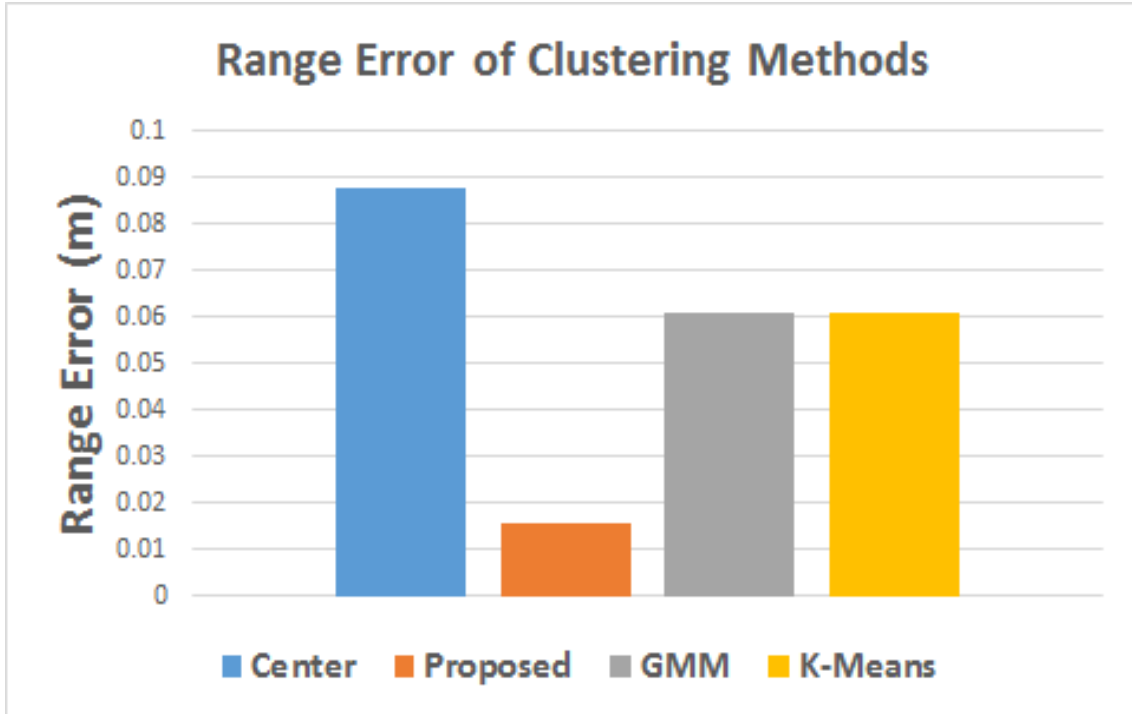


Figure 6. Range error between the actual object and the detected object

Figure 5 shows the detection rate according to the clustering methods using the low resolution LIDAR. Figure 6 indicates the distance error between the actual human position and the cluster position generated by the LIDAR. All clustering methods have the detection rate about 99 % in a single target environment, as shown in Figure 5. In Figure 6, the center is the central point of the line connected of the first point and the last point in the object cluster detected from LIDAR. The proposed algorithm has the fewest error which is difference between the actual human position and the central point of the cluster. The error calculated by the proposed algorithm of between the real object location and the central point is 0.015m. When the GMM and K-Means apply, the error has over 3 times compared to the HCF.

3.3. HCF Effectiveness

The experiments are performed for comparing other classification algorithms with the proposed algorithm, to assess the effectiveness of the proposed algorithm. The SVM and AdaBoost algorithm which require a variety of features and a plurality of data are not suitable because the low resolution LIDAR has the constrained features. The classification is performed in a single target and multi-target environment.

The upper boundary and a lower boundary with a shape pattern of the subjects are configured by the data set of the low resolution LIDAR. The shape patterns are extracted from front pose and side pose of the subjects. Figure 7 shows the patterns and the output dataset of the LIDAR used for the experiment. The pattern matching process is performed by the similarity of between the clusters and the configured pattern.

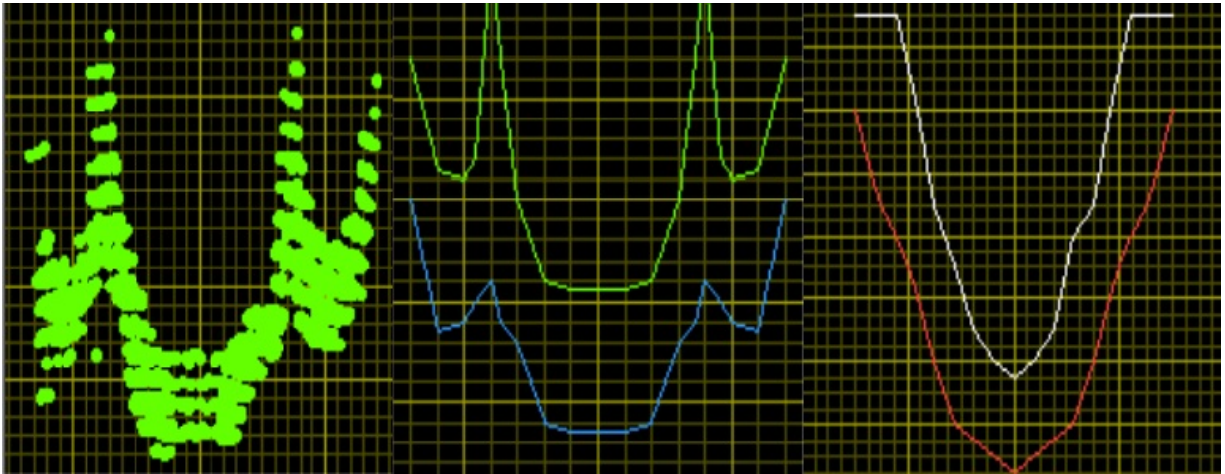


Figure 7. A human pattern from low resolution LIDAR dataset: (a) Human data cloud measured from LIDAR (b) A front pattern generated from cloud data (c) A side pattern generated from cloud data

The region of interest (ROI) is determined by the located area of the human in a single target environment without obstacles. Since the pattern matching algorithm depends on the results of the clustering, the detection rate is over 99% in a single target environment as shown in Figure 5. The upper figure of Figure 8 shows the LIDAR data. The yellow line in the upper figure of Figure 8 represents the field of view of the camera. Figure 8 shows a multiple target environment that is composed of one wall, three obstacles, and three human. The experiments are performed by comparing the proposed HCF with the distance-based clustering, GMMC, and K-Means using a pattern matching algorithm. The experimental results are shown in Figure 9. When the GMMC is applied to the pattern matching, its detection rate is lower than other algorithm. In the case of distance-based clustering algorithm, the first and the second human are detected with a probability of about 52% and 42%. However, the third human is not recognized. If K-Means is applied to the experiment, the first human adjacent from LIDAR is detected about 79%, and the second and the third human are discovered with the lowest probability.

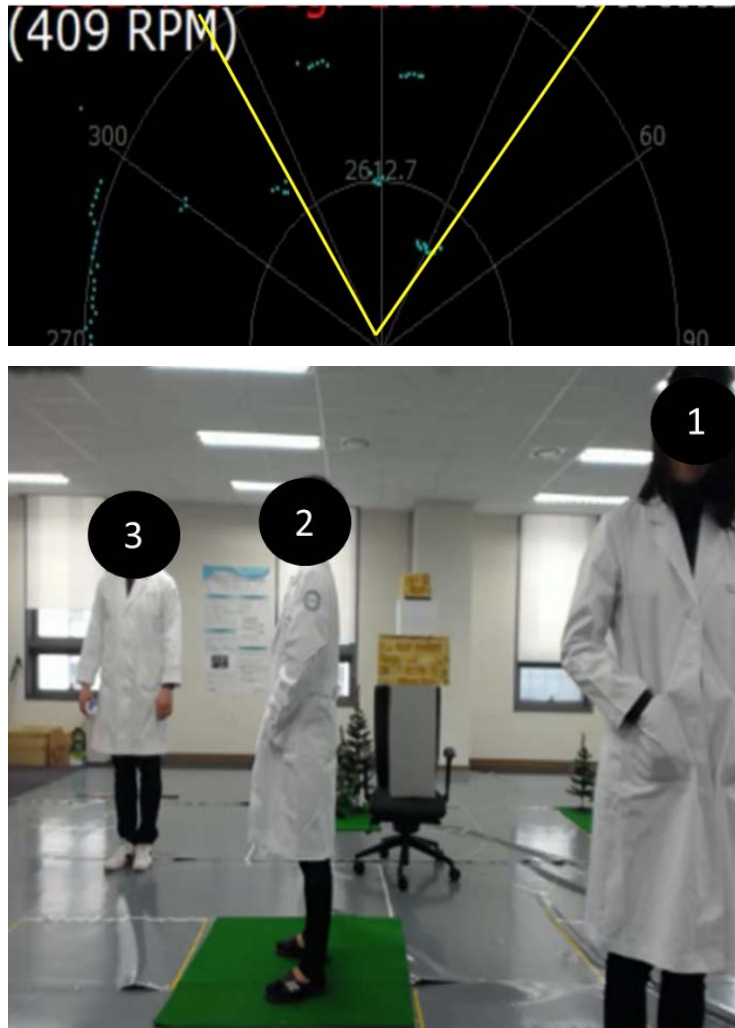


Figure 8. Multi-targets experiment environment

The results applying the proposed HCF have high performance compared to the other algorithms. The detection results of the first human located to 1.5m and the second human positioned to 3m are about 99% and about 98%. The third human is located in the most remote 4.5m, and it is detected about 57%. Therefore, the proposed method shows the best performance in the experiments applying the four algorithms. The detection rate of the third human has low performance than other human. The low detection rate is occurred as the lack of the output data that the human is located distantly from the sensor. In the results of the experiments, the effectiveness of the proposed

algorithm is verified as the detection performance of about 98% into a radius of 3m. However, if the detection range is exceeded, the detection rate decreases by the constraint of the LIDAR. The proposed HCF that is based on a quadratic polynomial curve shows the applicability of the human detection technology using low resolution LIDAR.



Figure 9. Multi-targets detection rate of the proposed algorithm and other clustering methods using pattern recognition

The performance of high resolution LIDAR [41] is referred in order to compare with the HCF. The detection rate provided from [41] is about 80%. In this case, the detection range of the LIDAR has the wide field of view of about 80m in comparison with LIDAR of this paper. In addition, the referred [41] applies the machine learning. Since the low resolution LIDAR lacks the output data, the utilization of the machine learning is difficult. However, the performance is similar to between

the method using the high resolution LIDAR and the proposed method. In addition, the proposed method has the virtue which is rapidly detecting the human compared to the learning method. Furthermore, the HCF is possible to apply to the method using the high resolution LIDAR as well as the low resolution LIDAR.

4. Conclusion

In this paper, we propose a method for quickly and easily detecting the human that is not sensitive to indoor or outdoor environment without machine learning. The previous human detection methods use the LIDAR which has high resolution and is expensive. However, even though the proposed method uses the low resolution LIDAR with inexpensive, it can obtain the features of the human precisely.

The proposed method for detecting the human is verified in the various experiments without machine learning. In addition, the effectiveness of recognizing the human is proved by the experiments via the HCF that is estimated by a quadratic polynomial curve from low resolution LIDAR data. However, the classification error which is occurred by similar obstacle with the human still remains in the 2D LIDAR. In addition, the study on the precise classification between the human and the obstacles which have features similar to the human is one of important challenges.

IV. Occluded Pedestrian Detection

1. Conventional Occluded Object Detection Systems

Conventional object detection technologies often employ a camera sensor because it can easily extract various features such as color, contour, and image pattern. However, these technologies have drawbacks such as heavy calculation burden and high sensitivity to the environment. In this paper, we use LIDAR and RADAR instead of a camera for occluded pedestrian detection as well as object detection. This section reviews the conventional sensor fusion technologies related to occlusion detection and object detection.

1.1 LIDAR-Camera Sensor Fusion

The technique to apply in LIDAR-Camera sensor fusion is occlusion reasoning methods. In the case of partially occluded objects, it is difficult to extract the characteristic features of a target accurately. Therefore, machine learning algorithms are utilized to infer the occluded object on the basis of sparse information. Typical occlusion reasoning methods are edge-contour based reasoning and frame comparison reasoning. Edge-contour based reasoning infers an object by means of its edge and contour of an occluded object [23-25]. Frame comparison reasoning uses a continuously input image dataset in accordance with time. This method determines the occlusion by analyzing the continuous image data. An occluded object is inferred by comparing the current and previous frames. This method is very effective for brief or instant occlusion. However, it is difficult to estimate consecutive occlusion because of storage is by a limited buffer size [26-27, 42]. These fusion methods still have a reliability problem due to the sensitivity to light change. In addition, it is difficult to detect a moving object. Therefore, to overcome this problem, LIDAR-

RADAR sensor fusion has been proposed to detect moving occluded objects with strong robustness to light change.

1.2 LIDAR-RADAR Sensor Fusion

A typical occlusion reasoning method using a LIDAR-RADAR sensor fusion is a modeling based method [43]. The vehicle measured from a LIDAR forms an L-shape. However, a partially obscured vehicle by other obstacles does not form a perfect L-shape. To construct an L-shape for a partially occluded vehicle, the Ramer algorithm was proposed in [44]. In addition, a vehicle is classified by using its width, length, and height measured from LIDAR [44-45]. These methods are good approaches to estimate vehicles in a clear environment because an L-shape can be reconstructed. However, they have some limitations to detect a pedestrian since humans have arbitrary shape.

In this paper, we propose a new and accurate detection method for pedestrians by means of a human characteristics curve based on LIDAR. We also introduce a new concept of occluded depth generation in order to determine if an occluded object exists or not.

2. Occluded Depth based Occlusion Reasoning Scheme

Figure 10 shows a concept of the proposed occluded pedestrian detection strategy. To compensate for the installment position difference between two sensors, calibration is performed for matching to the respective coordinate system in a pre-processing step. Typically, the LIDAR and RADAR ROIs of an object result from performing the respective detection algorithm. In the proposed algorithm, the occluded depth generation is newly introduced in the fusion processing step. The fusion ROI is produced by overlapping LIDAR ROI and RADAR ROI and it is used for estimating the precise position of an object. That is, LIDAR detects only the outermost objects and

does not detect any objects hidden by obstacles. The occlusion depth is generated in order to consider the possibility of any objects being hidden behind other objects. In addition, an occluded depth determines whether an occluded object exists within a fusion ROI. Furthermore, when an occluded object exists within an occlusion depth, it is estimated to be a pedestrian by obtaining the human Doppler distribution from RADAR. If an object is not obscured, classification is finally performed by using both the Doppler pattern measured from RADAR and the human characteristics curve extracted from LIDAR.

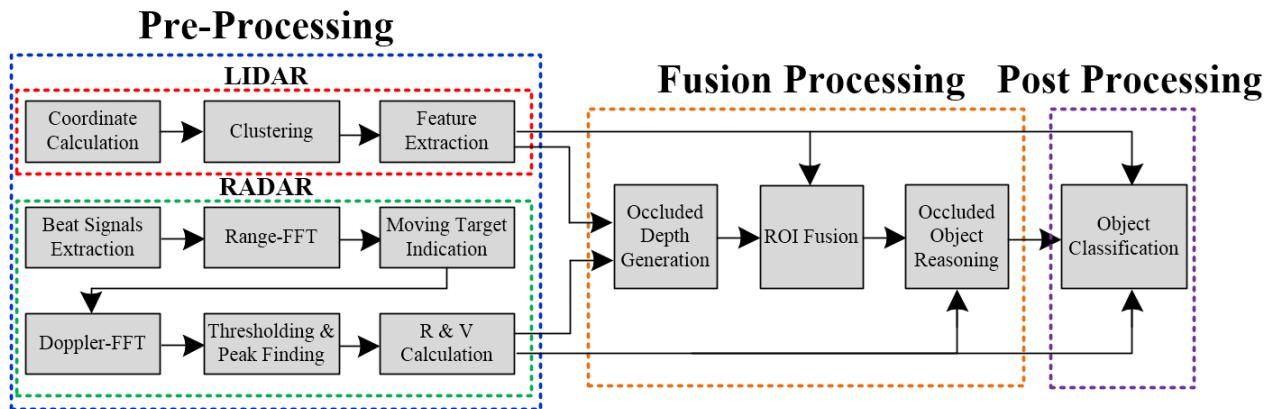
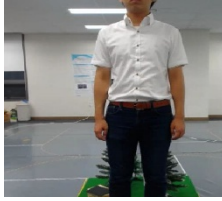
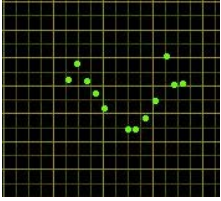
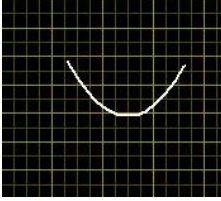
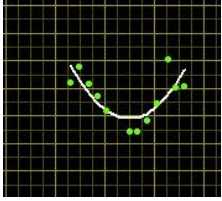
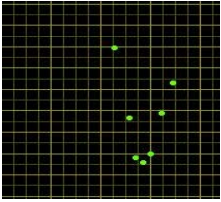
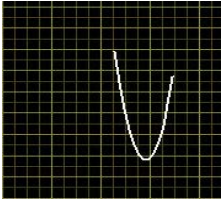
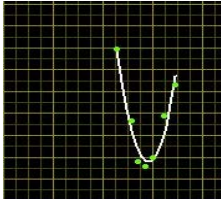
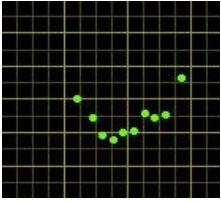
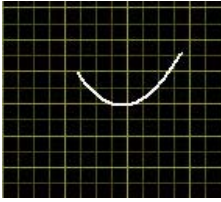
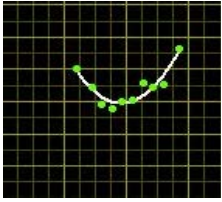


Figure 10. The proposed occluded object detection scheme using LIDAR and RADAR sensor fusion.

Table 1 shows a human body and a quadratic curve fitting measured by LIDAR. The human body observed by LIDAR has features forming a streamlined shape. In order to extract only the human features, LIDAR data are approximately fitted to a curved form with higher-order functions. If a human shape is approximately fitted to the first-order function, the fitting curve is inaccurately made. If a human shape is expressed by a 3rd or higher-order approximation, the fitting curve is similar to the features of other objects. However, if a human shape is fitted to the second-order curve fitting, a human has slope features that are distinguished from other objects. The proposed

method to classify a human on the basis of height, width, thickness, and tilt features is called the human characteristics curve technique.

Table 1. The human characteristics curve of typical human postures

Posture	Situation	LIDAR data	Fitting data	Overlay data
Front				
Side				
Back				

2.1 Object Detection

Object detection techniques are pre-processing steps for detecting an object with LIDAR and RADAR, respectively. LIDAR and RADAR perform object detection. A RADAR ROI is utilized to reduce the processing time in an object detection step.

A) LIDAR-Based Detection

The LIDAR model used in this study is Velodyne VLP-16, 3D LIDAR with 16 channels, in this study. The distance, angle, and height of an object are obtained from the LIDAR. Here, the processing data can be reduced by using spatial filtering in the region of interest.

$$\text{Channel MDR} = \text{LIDAR mounting position} \times \tan(90^\circ - \theta_{channel\ num}) \quad (5)$$

The maximum detection range per channel is calculated by Equation 5 according to the height and angle of LIDAR. The LIDAR process in Figure 10 is one of the object detection steps. The object measured from LIDAR appears as a group with scattering points. Through the clustering process, the distribution of scattering points is analyzed and the scattering points are combined into the same group. In this paper, a distance based method is used for a clustering process. The clustering method is to merge scattered points and nearest neighboring points into a bigger group when many scattered points are closely located within any predetermined threshold window. The threshold is calculated by a vector norm operation in accordance with distance. This clustering is used to extract the width, length, and height of an object.

B) RADAR-Based Detection

The RADAR used in the study has a fast-ramp based FMCW (Frequency Modulated Continuous Wave) waveform [30]. The fast-ramp based FMCW RADAR detects an object by transmitting ramp trains, which are modulated as a saw-tooth shape and by 2D FFT (Fast Fourier Transform) processing. The signal reflected from an object is sampled by means of an ADC (Analog Digital Converter). The sampled signal per ramp is transformed by the range-frequency spectrum through a range-FFT. Generally, the signal reflected from a pedestrian can be masked off due to strong surrounding clutter because a pedestrian has relatively low reflectance. Thus, a MTI (Moving Target Indication) removes clutter components and extracts only a moving object. A range-Doppler map is then built from Doppler-FFT processing. The object is finally extracted by finding peaks with an adaptive thresholding based on CA-CFAR (Cell Averaging Constant False Alarm Rate) in a 2D range-Doppler map. The obtained distance and velocity are the object

information in a RADAR ROI. The Doppler pattern of a pedestrian is obtained from Doppler-FFT processing [30].

2.2 Occluded Depth Generation based LIDAR and RADAR Sensor Fusion Scheme

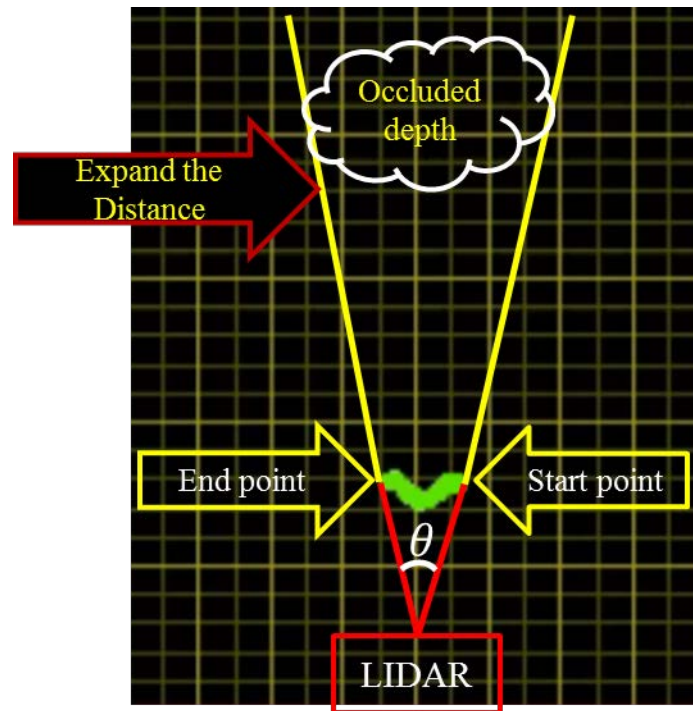


Figure 11. Occluded depth generation process

A typical method for a partially occlusion detection has been applied to estimate the contour of an object that is partially hidden by other barriers [23, 25]. However, this method requires a heavy computation burden. To solve this problem, we introduce a novel concept of occluded depth generation. The occluded depth is a shadow region, which means some regions are occluded but detected. Occluded objects can exist within the depth. As LIDAR detects the outermost object, the occluded depth is initiated at its position of the detected object from LIDAR. Thus, the beginning

and ending lines in the occluded depth are formed by the outermost end points of the LIDAR scattered cluster, as shown in the Figure 11.

A RADAR ROI is produced on the basis of RADAR range because RADAR has good longitudinal but bad horizontal resolution. However, LIDAR obtains the accurate position of an object due to good horizontal and longitudinal resolution. A LIDAR ROI is strongly dependent on the width and length of an object. ROI overlay is made by overlapping the ROIs of LIDAR and RADAR sensors and extracting the overlapped ROI region. As a result of ROI overlay, it is possible to obtain a precise fusion ROI or an occlusion ROI. The computation burden for occlusion reasoning becomes lighter since the fusion ROI is narrowed relative to the respective sensor ROI.

Figure 12 is a step-by-step procedure of an occluded depth generation based RADAR and LIDAR sensor fusion. Figure 12(a) is a snapshot picture showing a situation in which a pedestrian is obscured by another pedestrian. Figure 12(b) is the measured data from the LIDAR. Figures 12(c) and 12(d) are the RADAR ROI and LIDAR ROI, respectively. Here, the LIDAR detects only the front pedestrian because it does not detect any occluded objects. Figure 12(e) shows the occluded depth generated from the front object detected by LIDAR. Figure 12(f) shows the fusion ROI, which is a more precise ROI extracted by superimposing the occluded depth and the ROI of each sensor. Figure 12(g) is the final detection result obtained through the proposed sensor fusion strategy. The occluded pedestrian is inferred from the proposed procedure.

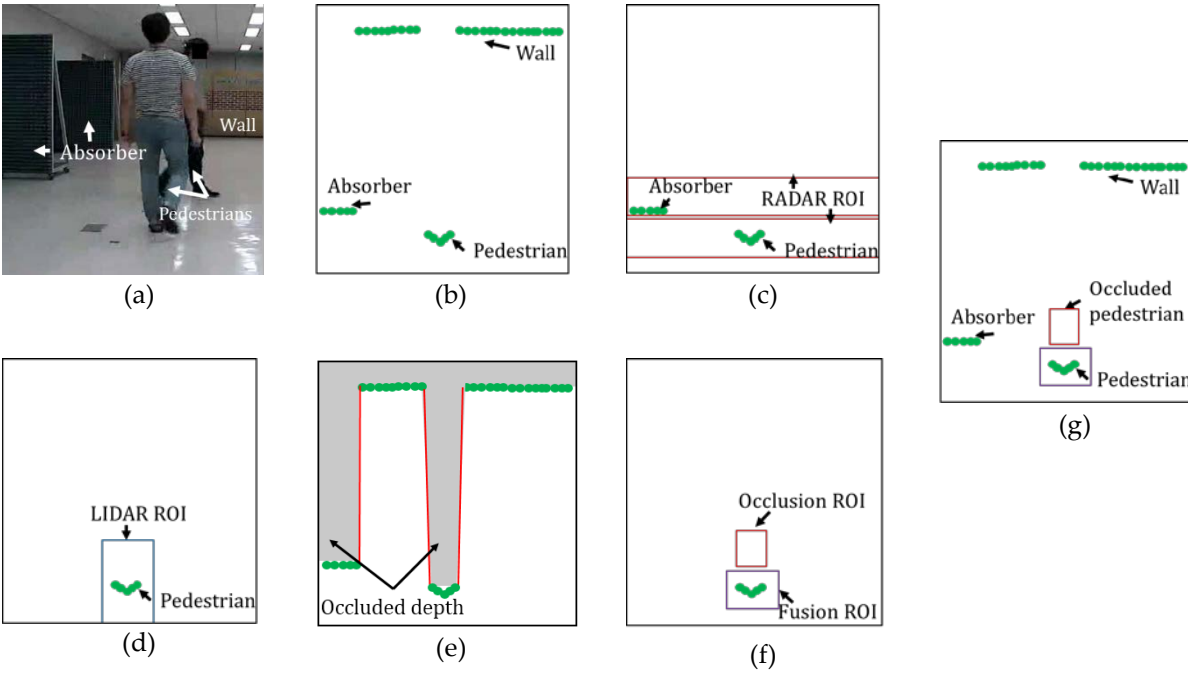


Figure 12. Occluded depth based LIDAR and RADAR sensor fusion scheme: (a) A snapshot picture of an occlusion situation, (b) The measured LIDAR data, (c) The estimated RADAR ROI, (d) The estimated LIDAR ROI, (e) The generated occluded depth, (f) The occlusion ROI and fusion ROI, and (g) The final sensor fusion result.

2.3 Occluded Object Reasoning and Classification

An occluded object reasoning is a process to recognize any object located inside the occluded depth. The occluded object reasoning utilizes the range, velocity, and Doppler pattern extracted from RADAR since LIDAR cannot obtain any obstacle information within the occluded depth. The occlusion ROI is obtained by using RADAR ROI and the occluded depth as mentioned above. The occluded object is inferred based on the information extracted from occlusion ROI inside RADAR. RADAR can detect a human walking even in an occlusion environment because RADAR is mounted inside the bumper of a vehicle, such as an unmanned vehicle. When a human walks, one leg is fixed and the other takes a step forward. During walking, a human Doppler

distribution is uniquely observed by moving and stationary patterns, repeatedly. This radar Doppler pattern is a human characteristic that is distinguishable from other obstacles [46]. Thus, this unique radar Doppler pattern is estimated to be a human.

If an object is outside from an occlusion region, an object is classified with the human characteristics features with the width, length, height, and slope obtained from LIDAR [6, 9, 47]. The cluster measured from LIDAR is fitted well to the second-order fitting curve since a human body can be modelled by a streamlined curve. The extracted information from each sensor is utilized to determine whether an object is a pedestrian. A pedestrian and other objects have different Doppler patterns [48], and a vehicle or motorcycle have a L-shape or I-shape instead of a streamlined shape [43]. The proposed method to detect an occluded pedestrian has low complexity because the method utilizes only the unique human features of LIDAR and RADAR instead of machine learning.

3. Experiment

3.1 Experimental Setup

Various experiments were carried out in indoor and outdoor environments to verify the performance of the proposed detection scheme. The experimental scenarios have been chosen in order to prove the effectiveness of the algorithm in a variety of environments.

Table 2. Their specifications of the used LIDAR and RADAR in experiments

Specification	LIDAR	RADAR
Type	903 nm laser	FMCW
# of channels	16	1
Maximum range (meter)	100	15
Field of View (horizontal)	360°	30°
Field of View (vertical)	30° (+15° to -	-
Center frequency (GHz)	-	24
Radial velocity (km/h)	-	+14 to -14
Sampling rate (MHz)	0.3	5

Table 2 shows the specifications of a Velodyne VLP-16 LIDAR and a 24GHz FMCW RADAR [49] used in the experiment. The RADAR was attached to the bumper position of a vehicle and the LIDAR was installed at about 2m height from the ground. This configuration is similar to that of an autonomous vehicle. Obstacles were located at approximately 2.2 times the mounting height of LIDAR. In addition, an experiment was performed to measure the detection accuracy by varying an obstacle's location corresponding to about 3, 4, and 5 times its height. The logging board and software developed by the present authors [50] are used to collect the measurement data of the RADAR.

The distance, velocity, and Doppler pattern of an object are measured from the RADAR and the measurement data of the LIDAR are gathered through Ethernet interface. They are used for the proposed pedestrian detection algorithm. Tables 3 and 4 summarize various experiment scenarios. The detection performance was evaluated in indoor and outdoor environments.

Table 3. Indoor environments of measurement scenarios

# of Scenarios	Environment	Situation	Schematics
i	Indoor Three absorber One pedestrian	<ul style="list-style-type: none"> ✓ No occlusion ✓ Forward direction ✓ Backward direction 	
ii	Indoor Three absorber One pedestrian	<ul style="list-style-type: none"> ✓ Fully occlusion ✓ Front side obstacle between 4.5m and 7.5m 	
iii	Indoor Three absorber One pedestrian	<ul style="list-style-type: none"> ✓ Partially occlusion ✓ Right side obstacle between 4.5m and 7.5m ✓ The pedestrian avoids the obstacle 	

Table 4. Indoor environments of measurement scenarios

# of Scenarios	Environment	Situation	Schematics
iv	Outdoor One tree One pedestrian	<ul style="list-style-type: none"> ✓ No occlusion ✓ Forward direction ✓ Backward direction 	<p style="text-align: center;">Scenario (iv)</p>
v	Outdoor One tree One obstacle One pedestrian	<ul style="list-style-type: none"> ✓ Fully occlusion ✓ Front side obstacle between 4.5m and 7.5m 	<p style="text-align: center;">Scenario (v)</p>
vi	Outdoor One tree One obstacle One pedestrian	<ul style="list-style-type: none"> ✓ Partially occlusion ✓ Right side obstacle between 4.5m and 7.5m ✓ The pedestrian avoids the obstacle 	<p style="text-align: center;">Scenario (vi)</p>

3.2 Experimental Results

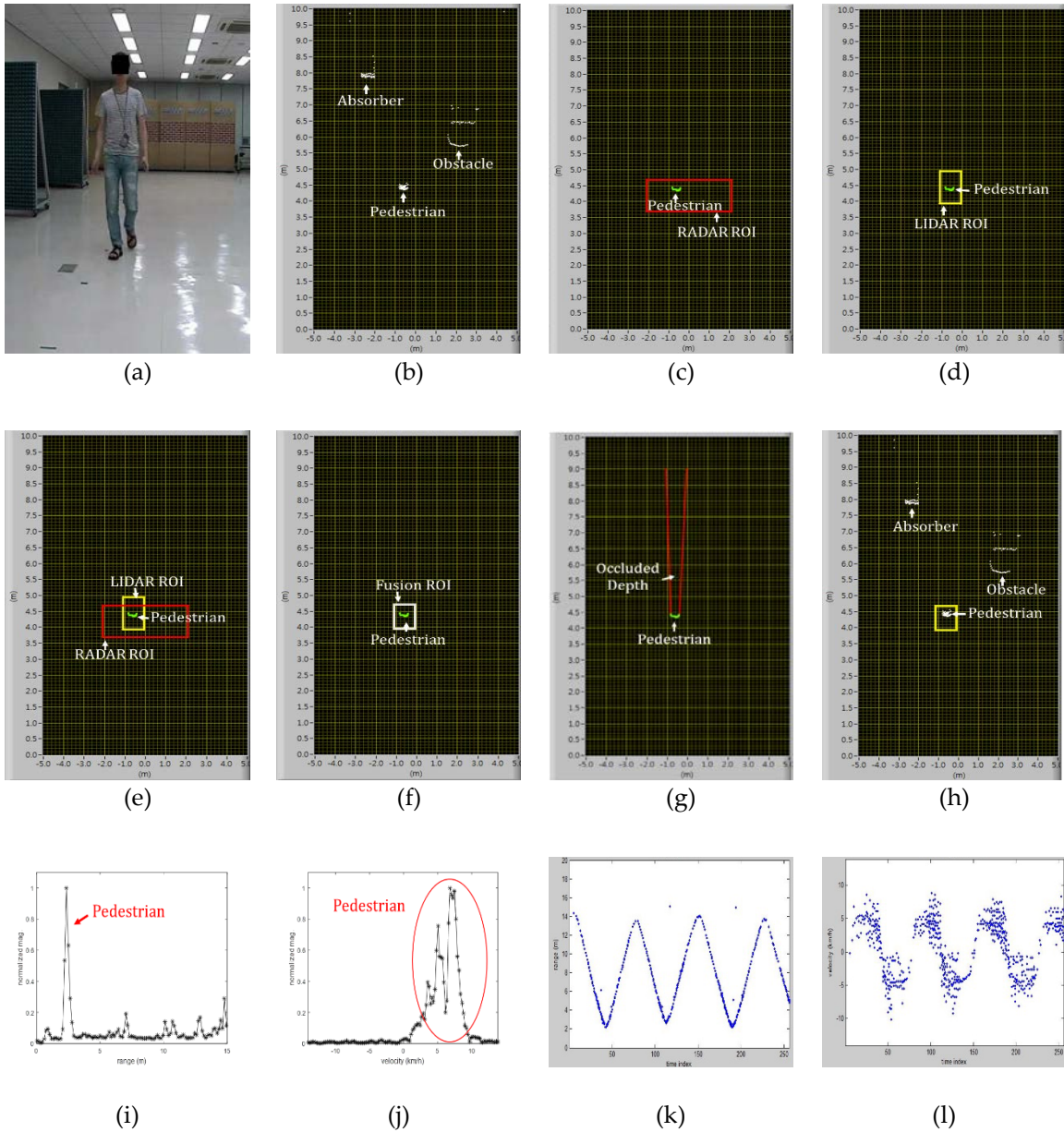


Figure 13. The experimental results in scenario (i): (a) Experimental environment, (b) The LIDAR measurement data, (c) The RADAR ROI, (d) The LIDAR ROI, (e) The ROI overlay for extraction of a fusion ROI, (f) The fusion ROI, (g) The occluded depth, (h) The final object detection result using the proposed sensor fusion, (i)The RADAR range spectrum (j) The RADAR velocity spectrum (k)The RADAR range variations of a pedestrian with time, and (l)The RADAR Doppler variations of a pedestrian with time.

Figures 13 to 18 show pedestrian detection results for six experiments. Scenario (i) is a situation showing that a pedestrian detection was carried out in an indoor open environment. In an open environment, as shown in Figure 13, a pedestrian was obviously measured in both the LIDAR and the RADAR, simultaneously. Figure 13(a) is the experimental situation based on the scenario (i). Figure 13(b) shows the measurement data extracted from the LIDAR. Here, the pedestrian could not be estimated through the clustering because the pedestrian and the absorber are very close to each other and they are not distinguished in this step. To classify the pedestrian in Figure 12(b), the RADAR ROI is needed, as shown in Figure 13(c), and the RADAR ROI is made on the basis of the detected distance. The horizontal boundary of the RADAR ROI is determined by the azimuthal coverage of RADAR. The vertical boundary of the ROI is set to a predetermined threshold that confines a pedestrian in [9]. As shown in Figure 13(c), a red rectangle is the RADAR ROI, and green points are the LIDAR data within the RADAR ROI. The green cluster is a moving object because the RADAR ROI includes a moving object detected from the RADAR. The LIDAR ROI is produced for detecting a pedestrian and it corresponds to a yellow rectangle in Figure 13(d). To obtain the precise position of an object, the fusion ROI is extracted by overlapping the RADAR ROI and LIDAR ROI, as shown in Figure 13(e). The resultant fusion ROI presents white squares, as shown in Figure 13(f). The occluded depth is generated from the detected object by the LIDAR, and it is expressed as a red line in Figure 13(g). In other words, the depth is projected out by expanding the longitudinal distance while maintaining the angle formed by the two outermost end points of the LIDAR scattered cluster. The proposed detection scheme results in detecting a pedestrian, as shown in Figure 13(f), since there are no barriers to hide a target in scenario (i). Here, to classify a pedestrian within the fusion ROI, the measured Doppler pattern extracted from

RADAR is used. Figures 13(i) and 13(j) show the RADAR range and Doppler spectra, respectively. The distance of a pedestrian is measured from the RADAR, as shown in Figure 13(i). Figure 13(j) is the velocity distribution of a pedestrian measured by RADAR. The measured instantaneous velocity has a broad distribution due to pedestrian movement. Figures 13(k) and 13(l) show the measured range and Doppler variations of a moving pedestrian along time, respectively. A pedestrian goes back and forth repeatedly in front of sensors. As depicted in Figure 13(l), the RADAR Doppler distribution is caused by the leg and arm sway during human movement. The Doppler pattern has a fairly repetitive pattern because, when a pedestrian moves, one leg is fixed and the other swings.

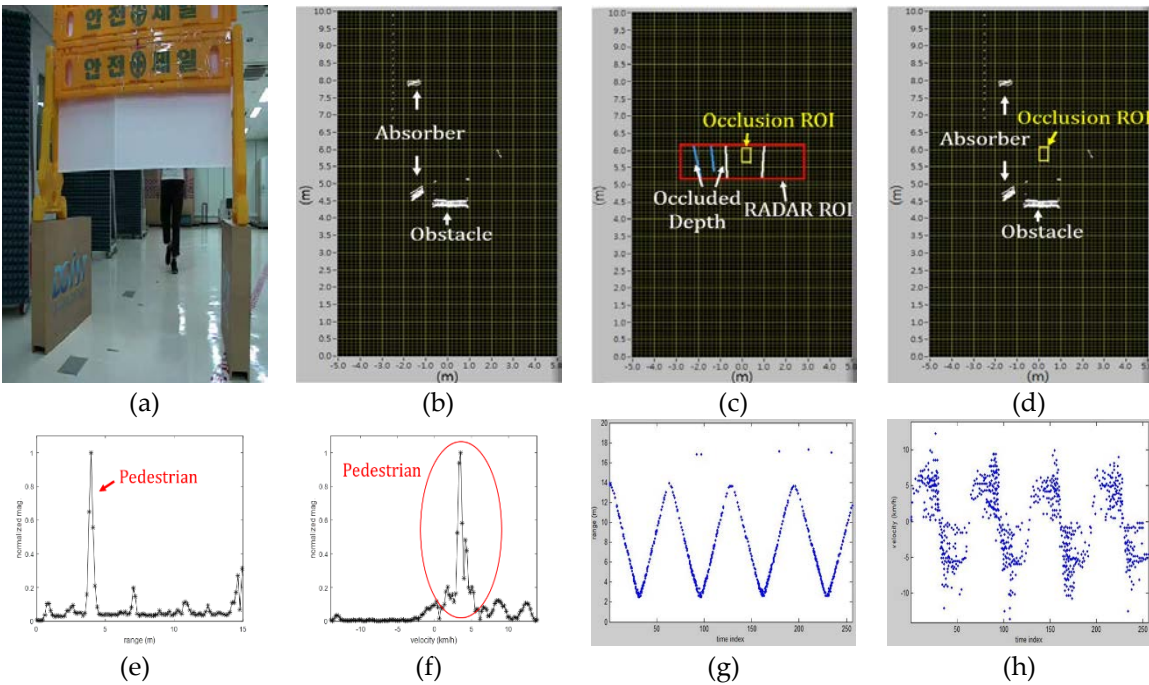


Figure 14. The pedestrian detection results in scenario (ii): (a) Experimental environment, (b) The LIDAR measurement data, (c) The RADAR ROI and the occlusion depth, (d) The occluded pedestrian detection result, (e) The RADAR range spectrum, (f) The RADAR Doppler spectrum, (g) The RADAR measured range variations of a pedestrian, and (h) The RADAR measured Doppler variations of a pedestrian.

Figure 14 shows an experiment of a partially occluded pedestrian in an indoor environment. Here, a pedestrian is moving behind an obstacle located about 4.5m away from the LIDAR. Figure 14(a) shows the experimental environment. The LIDAR could not detect a pedestrian because the pedestrian is obscured by an obstacle. Figure 14(b) is the LIDAR measurement data corresponding to one obstacle and two absorbers in the background of an indoor closed space. Actually, a pedestrian is hidden behind a barrier. Thus, the LIDAR could not detect the occluded pedestrian since the pedestrian is partially hidden. The RADAR ROI is represented as a red rectangle in Figure 14(c). No data are extracted from the LIDAR inside the RADAR ROI. In Figure 14(c), there are two occluded depths. One includes two white lines and the other two blue lines. The existence of an object needs to be determined within this occluded depth. The occluded depth is generated on the basis of the LIDAR ROI since there is an invisible object. An occluded object could exist within the yellow rectangle including two white lines. The final object detection results are shown in Figure 14(d). The occluded object is estimated to be a pedestrian by using the unique RADAR Doppler distribution caused by a pedestrian's leg sway. After reasoning, the occlusion ROI including an occluded pedestrian is marked on a LIDAR measurement map. Figures 14(e) and 14(f) show the RADAR measured range and velocity spectra of a partially occluded pedestrian, respectively. Figure 14(g) and Figure 14(h) are the measured range and velocity variations of a pedestrian along time in scenario (ii), respectively. You can see the unique broaden Doppler distribution of a pedestrian with time.

Figure 15(a) is a snapshot picture showing another partial occlusion situation temporarily in an indoor closed environment. Here, an obstacle is located in the right side and a pedestrian walks and is hidden suddenly, and then avoids an obstacle and keeps going. Figure 15(b) is the LIDAR measurement data including an obstacle and three absorbers. Figure 15(c) shows the occluded

depth and RADAR ROI. The red rectangle indicates the RADAR ROI. The occluded depths are two. One includes white lines and the other two blue lines. In addition, you can see two occluded depths that exist within the RADAR ROI. Object reasoning is just accomplished within the generated occluded depths. Only one of the two occluded depths, that closest to the RADAR measured range, is chosen. Figure 15(d) shows the estimated occluded ROI within the chosen occluded depth, as seen in the yellow rectangle. Figures 15(e) and 15(f) show the RADAR range and Doppler spectra. You can see a moving pedestrian and stationary obstacles. Figure 15(g) is a snapshot picture showing that a pedestrian is about to avoid obstacles. Figure 15(h) is the LIDAR measured data. Here, a pedestrian and several obstacles are clearly separated. Figure 15(i) shows the RADAR ROI and the LIDAR ROI. Here, the RADAR ROI and the LIDAR ROI are red and yellow rectangles, respectively. In the case of the conventional clustering methods, a pedestrian and obstacles are grouped into the same cluster. On the other hand, the proposed method distinguishes a pedestrian from adjacent closely located obstacles by using RADAR Doppler measurement and sensor fusion. Figure 15(j) shows the pedestrian detection result of the LIDAR and RADAR sensor fusion based on the RADAR Doppler distribution and the LIDAR human characteristics curve. Figures 15(k) and 15(l) are the RADAR range and Doppler spectra in scenario (iii), respectively. A pedestrian and obstacles in the range spectrum are merged and are indistinguishable. However, they are clearly separated in the Doppler spectrum. Figures 15(m) and 15(n) are the RADAR measured range and Doppler variations along time in a condition of pedestrian movement in scenario (iii), respectively.

To prove the effectiveness of the proposed method in outdoor as well as indoor environments, outdoor experiments were carried out. Figure 16 is the result of a pedestrian detection with no occlusions in a clear outdoor setting. Figure 16(a) is a real experimental environment, and a

pedestrian is located in front of the two sensors. Figure 16(b) is the measured LIDAR data. Here, two clusters are detected in a range of about 10.5m and about 13m, respectively. Figure 16(c) is the pedestrian detection result. A pedestrian is detected by applying the human characteristics curve within the fusion ROI. Figure 16(d) is the final pedestrian detection result obtained by combining the RADAR Doppler distribution and the LIDAR human characteristics curve. Figure 16(e) is the RADAR range spectrum. Here, two peaks correspond to a pedestrian and trees, respectively. Figure 16(f) is the RADAR Doppler spectrum. It is possible to observe the velocity corresponding to the moving pedestrian. Figures 16(g) and 16(h) are the measured range and Doppler variations along time, respectively.

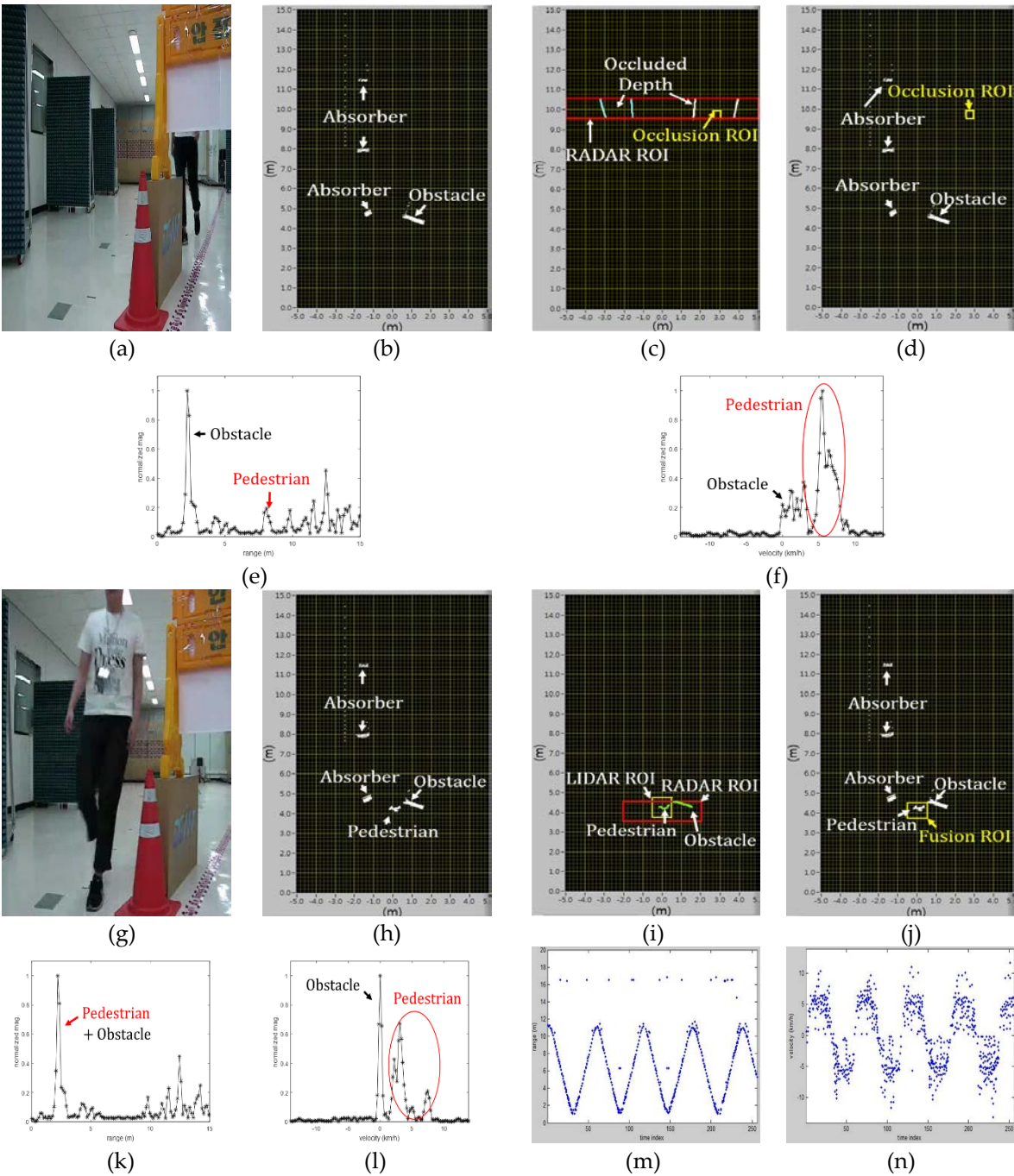


Figure 15. The pedestrian detection results in the scenario(iii): (a, g) Experimental snapshot pictures (b, h) The LIDAR measurement data, (c) Occlusion depth generation, (d) The occlusion ROI, (e) The RADAR range spectrum of an occluded pedestrian, (f)The RADAR Doppler spectrum of an occluded pedestrian, (i) The fusion ROI extraction result, (j) The occluded pedestrian detection result using fusion ROI, (k) The RADAR range spectrum of a pedestrian, (l) The RADAR velocity spectrum of a pedestrian, (m) The RADAR range variations of a pedestrian, and (n) The RADAR Doppler variations of a pedestrian.

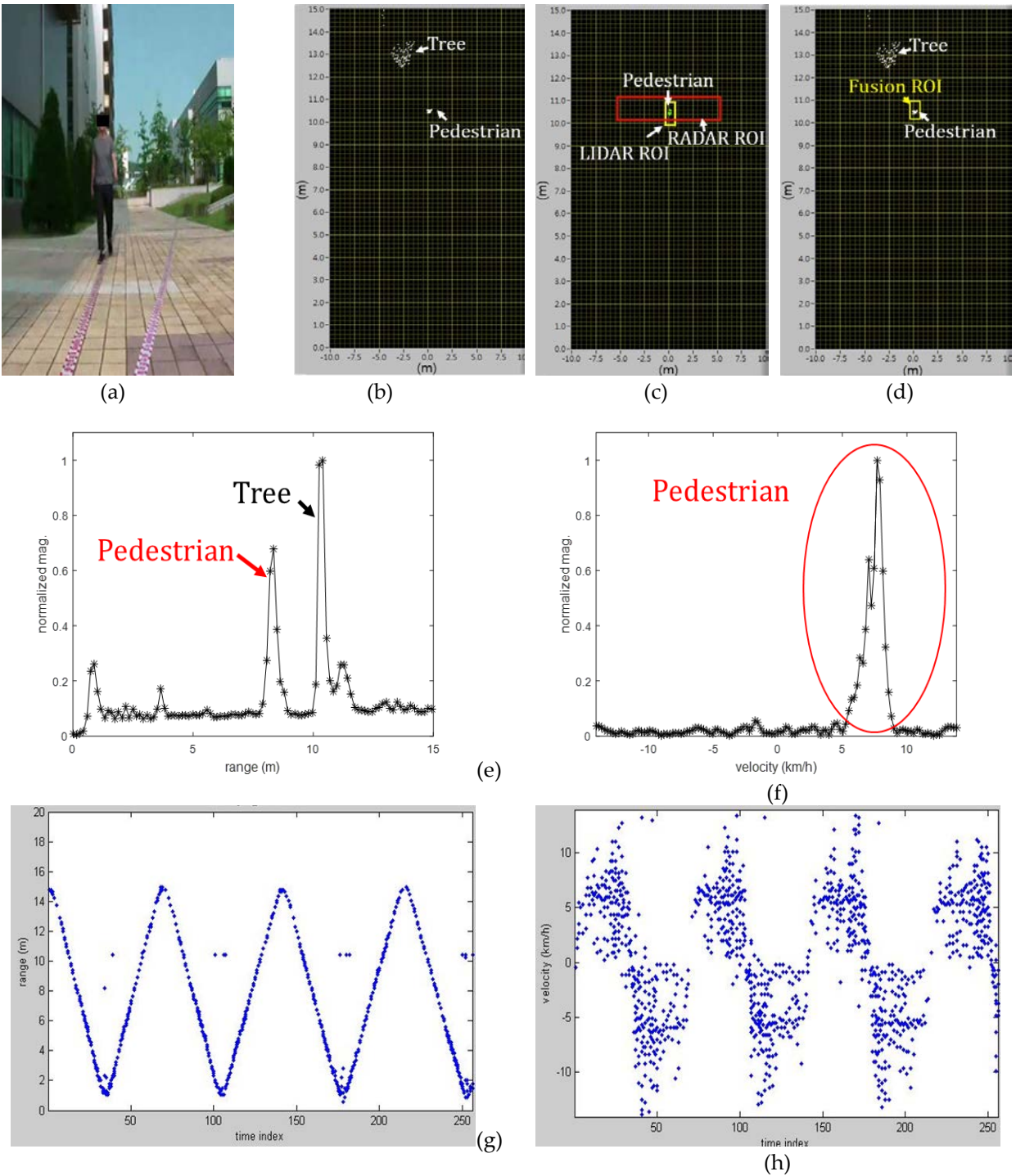


Figure 16. The experimental pedestrian detection results (iv): (a) A snapshot picture showing outdoor experimental environment, (b) The LIDAR measurement data, (c) The predicted RADAR and LIDAR ROIs, (d) The pedestrian detection result, (e) The measured RADAR range spectrum, (f) The measured RADAR Doppler spectrum, (g) The RADAR range variations of a pedestrian with time, and (h) The RADAR Doppler variations of a pedestrian with time.

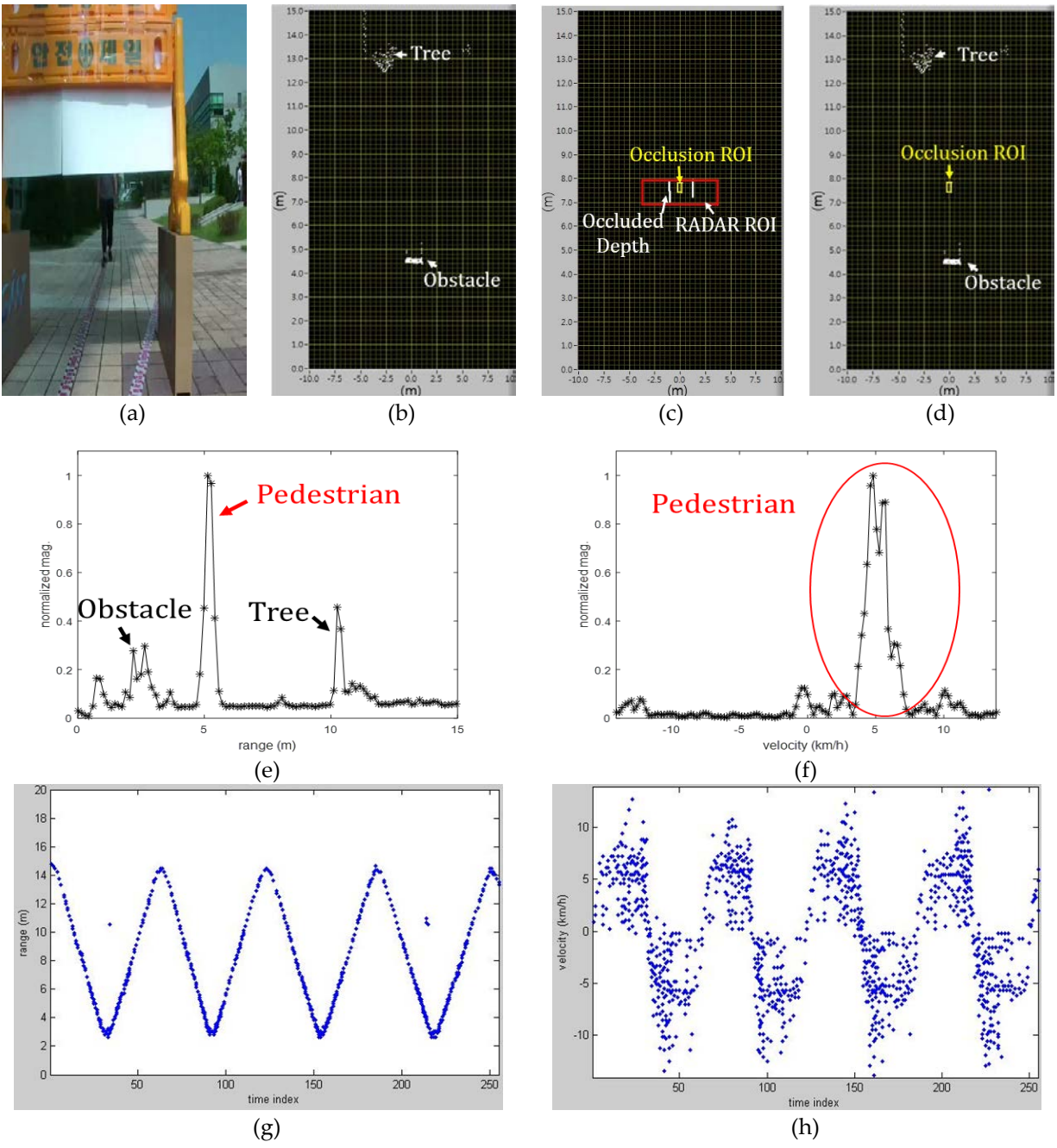


Figure 17. The experimental detection results in scenario(v): (a) A snapshot picture showing a partially occluded pedestrian in an outdoor experimental environment, (b) The LIDAR measurement data, (c) The occluded depth and the RADAR ROI, (d) The partially occluded pedestrian detection result, (e) The measured RADAR range spectrum, (f) The measured RADAR Doppler spectrum, (g) The RADAR range variations of a pedestrian with time, and (h) The RADAR Doppler variations of a pedestrian with time.

Figure 17 shows the pedestrian detection result in scenario (v). Figure 17(a) is a snapshot picture showing an outdoor occluded pedestrian situation. Here, a pedestrian is partially occluded. Figure 17(b) is the measured LIDAR data. The LIDAR does not detect the pedestrian due to the partial occlusion. Figure 17(c) shows the RADAR ROI and the occluded depth. The occluded pedestrian can be detected by overlapping the RADAR ROI and occluded depth. Figure 17(d) is the occluded object reasoning result using the RADAR Doppler distribution. Figure 17(e) is the RADAR measured range spectrum. The obstacles, trees, and a pedestrian are detected. Figure 17(f) is the RADAR measured Doppler spectrum. A broad peak is observed at velocity of about 5km/hr and this peak corresponds to an occluded pedestrian. Figures 17(g) and 17(h) are the RADAR range and Doppler variations along time in a condition that a pedestrian is moving with a partial occlusion, respectively. Figure 18 is the pedestrian detection results in an experiment in scenario (vi). Figure 18(a) is a real experiment picture. A pedestrian is occluded by the front barrier. Figure 18(b) is the LIDAR measurement data. In spite of the existence of a pedestrian behind obstacles, the pedestrian is not detected, as shown in Figure 18(b). Figure 18(c) is the occluded depth and the RADAR ROI extraction results. Here, the occlusion depth is generated within the RADAR ROI, and the occlusion ROI is confined by overlaying both the RADAR ROI and the occluded depth, as described in Figure 18(c). Figure 18(d) shows the inferred occluded pedestrian detection. Figures 18(e) and 18(f) are the RADAR measured range and Doppler spectra, respectively. Two peaks corresponding to obstacles and a pedestrian are clearly separated in the range spectrum and a broad peak at velocity of about 5km/hr is observed in the Doppler spectrum. Figure 18(g) is an experimental picture in the same scenario (vi). Figure 18(h) is the LIDAR measurement data. A pedestrian is detected close to the adjacent obstacle. Figure 18(i) is the estimated RADAR and LIDAR ROIs. Figure 18(j) is the fusion ROI and the final pedestrian detection result. A pedestrian

and its neighboring obstacles are separated by using the RADAR velocity information within a fusion ROI. Figures 18(k) and 18(l) are the measured RADAR range and Doppler spectra, respectively. A pedestrian and its neighboring obstacles in the range spectrum are merged because of the very small distance between them, as shown in Figure 18(k). However, a pedestrian is clearly distinguishable from stationary obstacles in the Doppler spectrum, as seen in Figure 18(l). Figures 18(m) and 18(n) show the RADAR measurement range and Doppler variations of a pedestrian movement in scenario (vi). The experimental Doppler distributions for a human movement in indoor and outdoor environments are very similar. We proved that the proposed method is very effective to detect a partially occluded pedestrian through various experiments.

The indoor and outdoor experimental results show that the proposed algorithm is very effective. The RADAR Doppler information and the LIDAR ROI are utilized to obtain the precise clustering of an object. In addition, a partially occluded pedestrian is determined within the occluded depth. Table 5 shows the pedestrian detection rate in various experimental situations based on the aforementioned scenarios. The experimental results based on scenario (i) and scenario (iv) reveal the same performance with and without the proposed method based on the occluded depth and sensor fusion because of the absence of barriers to occlude the pedestrian. On the other hand, a pedestrian is partially occluded in scenario (ii) and scenario (v). In scenario(ii), the detection rates without and with the proposed method are 8.1% and 89.5%, respectively, meaning the occluded depth based RADAR and LIDAR sensor fusion provides significant improvement in detecting a partially occluded pedestrian. A partially occluded pedestrian is not detected in the case without the proposed method in an outdoor scenario (v). The proposed sensor fusion scheme has a much higher detection rate of more than 89%. Also, scenario (iii) and scenario (vi) show much better detection performance by means of the LIDAR and RADAR sensor fusion scheme.

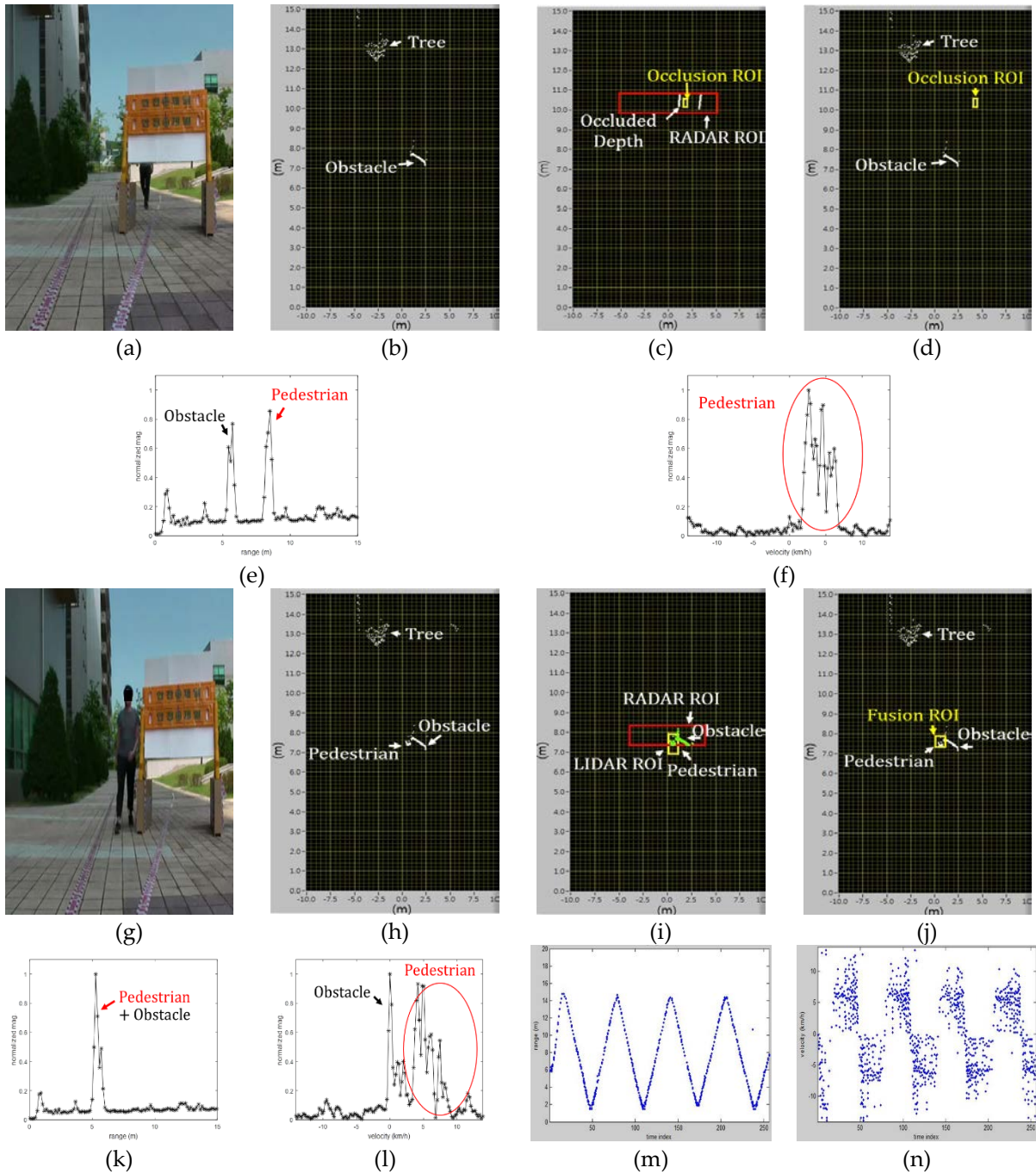


Figure 18. The experimental detection results in scenario (vi): (a and g) A snapshot picture showing an outdoor experimental environment, (b and h) The LIDAR Raw data, (c) The occluded depth and the RADAR ROI, (d) The partially occluded pedestrian detection result, (e) The measured RADAR range spectrum, (f) The measured RADAR Doppler spectrum, (i) The predicted fusion ROI, (j) The pedestrian detection result using the fusion ROI, (k) The measured RADAR Doppler spectrum, (l) The measured RADAR Doppler spectrum, (m) The RADAR range variations of a pedestrian with time, and (n) The RADAR Doppler variations of a pedestrian with time.

Table 5. Detection rate for each scenarios

		Scen	Scen	Scen	Scen	Scen	Scen
		ario (i)	ario (ii)	ario (iii)	ario (iv)	ario (v)	ario (vi)
Pedestrian detection rate	With out proposed Method	97.6 %	8.1 %	14.7 %	92.2 %	0 %	15.3 %
	With proposed method	97.6 %	89.5 %	97.6 %	92.2 %	95.7 %	92.3 %
Total frame		868	645	681	440	491	348

4. Conclusion

The proposed method is a new scheme to detect a partially occluded pedestrian by using occluded depth based LIDAR-RADAR sensor fusion. Generally, in an occlusion reasoning technique, a LIDAR and camera have been used for pedestrian detection. However, the camera is very sensitive to light intensity and environmental change. In addition, the occlusion reasoning in image processing imposes a heavy computation burden and much more processing complexity. To reduce the object detection computation, spatial filtering before the sensor fusion processing is applied. The proposed method introduces a new concept of occluded depth that is projected out from the outermost obstacles in order to determine whether an occluded object exists. When an object is hidden by obstacles, it is difficult for LIDAR to detect an occluded object whereas RADAR detects a partially obscured object. In particular, a moving object is detected well due to the Doppler pattern. The occluded depth based on LIDAR-RADAR sensor fusion detects a partially occluded pedestrian by combining the LIDAR human characteristics curve and the RADAR Doppler distribution of a pedestrian. The LIDAR characteristics curve is used for

distinguishing a pedestrian from other objects within the LIDAR ROI. The fusion ROI is generated by overlapping the RADAR and LIDAR ROIs and reduces the computation burden due to the precise and narrower ROIs.

In this paper, various experiments to detect a partially occluded pedestrian are performed in outdoor as well as indoor environments. According to the experimental results, the proposed sensor fusion scheme has much better detection performance compared to the case without the proposed method.

This sensor fusion scheme will be very useful in the autonomous vehicle field because hidden pedestrians can be detected in advance before a collision occurs.

V. Summary and Future Work

Human detection technologies have been applied in wide research area for safety and convenience. A variety of the sensors are used for the human detection. The human detection technologies applied in the smart home utilize a camera, ultrasonic, and motion sensor. However, these sensors have vulnerabilities of the detection which is the problems of deployment, sensitivity as environment, and complexity of algorithm. Furthermore, the pedestrian detection in autonomous vehicle area is most critical issue. The previous pedestrian detection utilizes the camera and the LIDAR. However, the sensitivity and classification problem still remain. In addition, conventional pedestrian detection technologies cannot detect a partially occluded pedestrian because of the lack of the sensor data. To address the problem, we propose the human characteristic based on human detection method and the occluded pedestrian detection method using the LIDAR.

The human characteristic function is represented by a quadratic polynomial curve because the human body has the streamline shape. To extract the feature, 2D low resolution LIDAR is used in this paper. The high resolution LIDAR has the improved measurement performance compared to low resolution LIDAR. However, the high resolution LIDAR is inappropriate the human detection in indoor environment because it has expensive complexity of classification. The low resolution LIDAR cannot obtain the precise feature of the human. Therefore, the application of the machine learning algorithm is difficult to detect the human. On the other hand, the HCF is possible to detect the human by the correction using a quadratic polynomial curve. The HCF provides the feature of the width, length, and slope information of the object. The human is estimated by these features.

The experiments results provide the comparison of the detection accuracy according to the polynomial degree and other algorithms respectively.

Another proposed method is partially occluded pedestrian detection based occluded depth generation. Generally, in an occlusion reasoning technique, a LIDAR and the camera have been used for the pedestrian detection. However, a camera is very sensitive according to light intensity and environmental change. In addition, the occlusion reasoning in an image processing requires heavy computation and much processing complexity. The spatial filtering before the sensor fusion processing is applied to reduce object detection performance. The proposed method introduces a novel concept of the occluded depth that is projected out from the most outer obstacles in order to determine whether an occluded object exists or not. When an object is hidden by any obstacles, it is difficult for a LIDAR to detect an occluded object but RADAR detects a partially obscured object. Especially, a moving object has very good detection due to the Doppler pattern. The occluded depth based on LIDAR-RADAR sensor fusion detects a partially occluded pedestrian by combining the LIDAR human characteristics curve and the RADAR Doppler distribution of a pedestrian. The LIDAR characteristics curve is used for distinguishing a pedestrian from other objects within the LIDAR ROI. The fusion ROI is generated by overlapping the RADAR and LIDAR ROIs and reduces the computation burden due to the precise and narrower ROIs. In this paper, various experiments are performed in detecting a partially occluded pedestrian in outdoor as well as indoor environments scenarios. According to experimental results, the proposed sensor fusion scheme has much better detection performance compared to the case without the proposed method.

The proposed algorithms are possible to apply a variety field such as smart home, mobile robot, and autonomous vehicle. The HCF will provide as convenience services based on the human detection. In addition, the proposed sensor fusion scheme will be very useful in an autonomous vehicle field because a hidden pedestrian can be detected in advance before a collision happens.

In the future, we will improve the detection performance of the pedestrian moved to horizontal using LIDAR and RADAR sensor fusion. Currently, autonomous vehicle is difficult to avoid the object because of lack of path planning and decision making. The erroneous control of the vehicle leads to collide between the vehicle and pedestrian. Therefore, we will challenge the decision making technique for pedestrian safety in autonomous vehicle.

REFERENCE

- [1] H. Zheng, H. Wang, N. Black, "Human activity detection in smart home environment with self-adaptive neural networks," in Proc. IEEE Int. Conf. Netw. Sensing Control, pp.1505-1510, 2008.
- [2] Aharon Bar Hillel, Ronen Lerner, Dan Levi, Guy Raz, "Recent progress in road and lane detection: a survey," Machine Vision and Applications, Journal, Vol. 25, Issue. 3, pp. 727-745, 2014
- [3] Christian Wojek, Stefan Walk, Stefan Roth, Konrad Schindler, Bernt Schiele, "Monocular visual scene understanding: Understanding multi-object traffic scenes." IEEE transactions on pattern analysis and machine intelligence, IEEE, Vol.35, Issue.4, pp. 882-897, 2013.
- [4] D. Zhang, F. Xia, Z. Yang, L. Yao, W. Zhao, "Localization technologies for indoor human tracking," in Future Information Technology (FutureTech), 2010 5th International Conference on. IEEE, pp.1-6, 2010.
- [5] M. Quigley, D. Stavens, A. Coates, and S. Thrun, "Sub-meter indoor localization in unmodified environments with inexpensive sensors," Intelligent Robots and Systems (IROS), 2010.
- [6] C. Premebida, G. Monteiro, U. Nunes, P. Peixoto, "A lidar and vision-based approach for pedestrian and vehicle detection and tracking," Intelligent Transportation Systems Conference (ITSC), IEEE, pp. 1044-1049, 2007
- [7] National Highway Traffic Safety Administration. National pedestrian crash report. Washington, DC: National Highway Traffic Safety Administration; 2015. Available at <http://www-nrd.nhtsa.dot.gov/Pubs/812124.pdf>
- [8] European Commission, Directorate-General Mobility and Transport, Unit C.4 – Road Safety: 2015. Available at http://ec.europa.eu/transport/road_safety/pdf/vademecum_2015.pdf
- [9] K. Kidono, T. Miyasaka, A. Watanabe, T. Naito, "Pedestrian recognition using high-definition LIDAR," Intelligent Vehicles Symposium (IV), IEEE, pp. 405-410, 2011
- [10] Aharon Bar Hillel, Ronen Lerner, Dan Levi, Guy Raz, "Recent progress in road and lane detection: a survey," Machine Vision and Applications, Journal, Vol. 25, Issue. 3, pp. 727-745, 2014
- [11] Christian Wojek, Stefan Walk, Stefan Roth, Konrad Schindler, Bernt Schiele, "Monocular visual scene understanding: Understanding multi-object traffic scenes." IEEE transactions on pattern analysis and machine intelligence, IEEE, Vol.35, Issue.4, pp. 882-897, 2013.

- [12] E. Osuna, R. Freund, F. Girosi, "Training support vector machines: An application to face detection," *Computer Vision and Pattern Recognition, IEEE*, pp. 130-136, 1997
- [13] Cao Xian-Bin, Qiao Hong, J. Keane, "A low-cost pedestrian-detection system with a single optical camera," *Transactions Intelligent Transportation Systems, IEEE*, Vol. 9, Issue. 1, pp. 58-67, 2008
- [14] Cheng Hong, Zheng Nanning, Qin Junjie, "Pedestrian detection using sparse gabor filter and support vector machine," *Intelligent Vehicles Symposium (IV), IEEE*, pp. 583-587, 2005
- [15] Wang, Xiaoyu, Tony X. Han, and Shuicheng Yan. "An HOG-LBP human detector with partial occlusion handling." *Computer Vision, 2009 IEEE 12th International Conference on*. IEEE, 2009.
- [16] Kong Dan, D. Gray, Tao Hai, "A viewpoint invariant approach for crowd counting," *International Conference Pattern Recognition (ICPR), IEEE*, pp. 1187-1190, 2006
- [17] F. Zhang, D. Clarke, A. Knoll, "Vehicle detection based on lidar and camera fusion," in *Intelligent Transportation Systems, 2014. ITSC 2014. 17th International IEEE Conference on*, pp.1620-1625. 2014.
- [18] M. Butenuth, F. Burkert, F. Schmidt, S. Hinz, "Integrating pedestrian simulation, tracking and event detection for crowd analysis," *International Conference on Computer Vision Workshops (ICCVW), IEEE*, pp.150-157, 2011.
- [19] C. Premebida, O. Ludwig, U. Nunes, "Lidar and vision-based pedestrian detection system," *Journal of Field Robotics*, vol. 26, no. 9, pp.696-711, 2009.
- [20] C. Premebida, O. Ludwig, U. Nunes, "Exploiting lidar-based features on pedestrian detection in urban scenarios," *Intelligent Transportation Systems Conference (ITSC), IEEE*, pp. 1-6, 2009
- [21] Daniel Gohring, Miao Wang, Michael Schnurmacher, Tinosch Ganjineh, "'Radar/lidar sensor fusion for car-following on highways." *Automation, Robotics and Applications (ICARA), IEEE*, pp. 407-412, 2011
- [22] C. Blanc, L. Trassoudaine, J. Gallice, "EKF and particle filter track-to-track fusion_ a quantitative comparison from radar,lidar obstacle tracks," *International Conference on Information Fusion, IEEE*, 2005
- [23] A. Yilmaz, Li Xin, M. Shah, "Contour-based object tracking with occlusion handling in video acquired using mobile cameras," *Transactions Pattern Analysis and Machine Intelligence, IEEE*, pp. 1531-1536, 2004.

- [24] M. Zeeshan Zia, Michael Stark, Konrad Schindler, "Explicit occlusion modeling for 3d object class representations," IEEE Conference on Computer Vision and Pattern Recognition, pp. 3326-3333, 2013.
- [25] Nadia Payet, Sinisa Todorovic, "From contours to 3d object detection and pose estimation," International Conference on Computer Vision, IEEE, pp. 983-990, 2011.
- [26] Zhou Yue, Tao Hai, "A background layer model for object tracking through occlusion," Computer Vision, IEEE, pp. 1079-1085, 2003
- [27] Lin Shin-Ping, Chen Yuan-Hsin, Wu Bing-Fei, "A Real-Time Multiple-Vehicle Detection and Tracking System with Prior Occlusion Detection and Resolution, and Prior Queue Detection and Resolution," International Conference Pattern Recognition (ICPR), IEEE, pp. 828-831, 2006
- [28] Sonia, Achyut Mani Tripathi, Rashmi Dutta Baruah, Shivashankar B. Nair, "Ultrasonic sensor-based human detector using one-class classifiers," International Conference on Evolving and Adaptive Intelligent Systems (EAIS), IEEE, pp. 1-6, 2015.
- [29] Chi-Wen Lo, Kun-Lin Wu, Jing-Sin Liu, "Wall following and human detection for mobile robot surveillance in indoor environment," International Conference on Mechatronics and Automation (ICMA), IEEE, pp. 1696-1702, 2014.
- [30] E. Hyun, Y. S. Jin, J. H. Lee, "A Pedestrian Detection Scheme Using a Coherent Phase Difference Method Based on 2D Range-Doppler FMCW Radar," Sensors, Vol. 16, no. 1, 2016
- [31] Han Jaehyun, Kim Dongchul, Lee Minchae, Sunwoo Myoungcho, "Enhanced road boundary and obstacle detection using a downward-looking LIDAR sensor," Transactions Vehicular Technology, IEEE, pp. 971-985, 2012
- [32] D. Gohring, Wang Miao, M. Schnumacher, T. Ganjineh, "Radar_lidar sensor fusion for car-following on highways," International Conference on Automation, Robotics and Applications (ICARA), IEEE, pp. 407-412, 2011
- [33] Jim Holilinger, Brett Kutscher, Ryan Close, "Fusion of lidar and radar for detection of partially obscured objects," SPIE Defense+ Security. International Society for Optics and Photonics, pp. 946806-946806-9, 2015.
- [34] Na Kiin, Byun Jaemin, Roh Myongchan, Seo Beomsu, "Fusion of multiple 2D LiDAR and RADAR for object detection and tracking in all directions," International Conference on Connected Vehicles and Expo (ICCVE), pp. 1058-1059, 2014
- [35] C. Blanc, L Trassoudaine, Y Le Guilloux, "Track to track fusion method applied to road obstacle detection," International Conference on Information Fusion, 2004

- [36] T. Ogawa, H. Sakai, Y. Suzuki, K. Takagi, K. Morikawa, "Pedestrian detection and tracking using in-vehicle lidar for automotive application," in Intelligent Vehicles Symposium (IV). IEEE, pp.734-739, 2011
- [37] L. Oliveira, U. Nunes, "Context-aware pedestrian detection using lidar," Intelligent Vehicles Symposium (IV), IEEE, pp.773-778. 2010.
- [38] K.O. Arras, Óscar Martínez Mozos, W. Burgard, "Using boosted features for the detection of people in 2d range data," in Proc. of the IEEE Int. Conference on Robotics and Automation, pp.3402-3407, 2007.
- [39] C. Premebida, U. Nunes, "A Multi-Target Tracking and GMM-Classifer for Intelligent Vehicles". Proc. of the IEEE ITSC 2006 IEEE Intelligent Transportation Systems Conference Canada, pp.313-318, 2006.
- [40] F. Morsdorf, E. Meier, B. Kötz, K. Itten, M. Dobbertin, B. Allgöwer, "LIDAR based geometric reconstruction of boreal type forest stands at single tree level for forest and wildland fire management", Remote Sens. Environ, vol. 92, no. 3, pp.353-362, 2004.
- [41] M. Lee, S. Hur, Y. Park, "Obstacle Classification Method Based on Single 2D LIDAR Database." IEMEK Journal of Embedded Systems and Applications, vol. 10, no. 3, pp.179-188, 2015(in Korean).
- [42] A. Faro, D. Giordano, C. Spampinato, "Adaptive Background Modeling Integrated With Luminosity Sensors and Occlusion Processing for Reliable Vehicle Detection," Transactions Intelligent Transportation Systems, IEEE, pp. 1398-1412, 2011
- [43] F. Nashashibi, A. Bargeton, "Laser-based vehicles tracking and classification using occlusion reasoning and confidence estimation," Intelligent Vehicles Symposium (IV), IEEE, pp. 847-852, 2008
- [44] U. Ramer, "An Iterative Procedure for Polygonal Approximation of Planes Curves", Computer Graphics and Processing, no. 1, pp. 244-256, 1972
- [45] Attila Bórcs, Balázs Nagy, Milán Baticz, Csaba Benedek, "A model-based approach for fast vehicle detection in continuously streamed urban LIDAR point clouds," Asian Conference on Computer Vision. Springer International Publishing, pp. 413-425, 2014.
- [46] Youngwook Kim, Sungjae Ha, Jihoon Kwon, "Human detection using Doppler radar based on physical characteristics of targets." IEEE Geoscience and Remote Sensing Letters, Vol. 12, no. 2, pp. 289-293, 2015.

- [47] Cheng Hong, Zheng Nanning, Qin Junjie, "Pedestrian detection using sparse gabor filter and support vector machine," Intelligent Vehicles Symposium (IV), IEEE, pp. 583-587, 2005
- [48] Rohling, Hermann, Steffen Heuel, Henning Ritter, "Pedestrian detection procedure integrated into an 24 GHz automotive radar." 2010 IEEE Radar Conference. IEEE, 2010.
- [49] Eugin Hyun, Youngseok Jin, Jonghun Lee, "Development of 24GHz FMCW level measurement radar system," IEEE Radar conference, IEEE, pp. 796-799, 2014
- [50] Youngseok Jin, Yeonghwan Ju, Sangdong Kim, Eugin Hyun, Jonghun Lee, "Implementation of the Real Time Data Logging System for Automotive Radar Development," International Symposium on Embedded Technology (ISET), Korea, 2016

요약문

라이다-레이더 센서 융합을 이용한 새로운 사람 탐지 방법 및 가려짐 추론

사람 탐지 기술은 널리 스마트 가정 및 자율 차량에 사용됩니다. 또한, 객체 탐지는 자율 차량에 보행자와 운전자의 안전을 위한 중요한 기술이다. 그러나, 사람을 검출하기 위해, 자동 운전 차량의 연구자들은 고해상도 라이다를 사용하고, 스마트 홈 연구자들은 좁은 검출 범위를 갖는 카메라를 적용했다. 객체 검출의 정확도를 개선하기 위한 센서 및 센서 퓨전 기술의 발전에도 불구하고, 가려진 보행자 검출 기술은 여전히 도전적인 분야이다. 기존의 가려진 보행자 탐지는 색깔과 윤곽 등의 다양한 특성을 추출하는 카메라를 이용한다. 그러나, 카메라는 환경 변화에 민감하고, 복잡한 영상 처리를 수행한다. 기존의 라이다와 레이더 융합 방법은 도플러 효과를 이용하여 물체들의 속도를 추정 할 수 있기 때문에, 이동하는 차량을 감지하는 데 사용되어왔다. 또한, 융합 방법은 환경 변화 및 기상 조건에 강력하다. 또한, 라이다와 레이더 융합 방법을 이용하여 폐색 된 보행자 검출 연구는 아직 초기단계이다. 이전의 폐색 보행자 감지를 위한 연구는 빛에 민감하고 복잡한 영상 처리를 수행하는 카메라 기반의 방법을 사용한다. 이러한 문제를 해결하기 위해, 우리는 라이다와 레이더 센서 융합을 이용한 새로운 폐색 깊이 생성 기반의 추론 방법을 제안한다. 인간을 분류하기 위해, 우리는 부수적인 학습 알고리즘과 추가적인 장치 없이 빠르고 정확하게 인간을 검출 할 수 있는 저가의 저해상도 라이다를 사용하는 새로운 방법을 제안한다. 즉, 인간의 몸의 형상에서 추출 된 새로운 인간 특성 함수를

이용하여 객체를 구별 한다. 또한, 제안하는 방법은 가려진 물체의 검출, 폐색 깊이 생성과 보행자 검출 단계로 구성된다. 폐색 깊이의 생성은 장애물에 의해 가려진 영역을 찾을 수 있는 방법입니다. 폐색 깊이 내부의 객체는 레이더에 의해 검출되고, 특별한 사람의 도플러 분포에 의해 보행자로 추정된다. 또한, 제안하는 방법은 각 센서의 관심 영역을 결합하여 정밀한 융합 관심 영역을 생성하기 때문에, 기존의 학습 방법 보다 비교적 낮은 연산량을 가진다. 따라서, 가려진 보행자는 레이더의 도플러 패턴, 라이더의 사람 특성 곡선 및 융합 관심 영역을 이용하여 추론될 수 있다. 또한, 우리는 다수의 실험을 통하여 제안하는 알고리즘의 효과를 검증하였다.

핵심어: 보행자 감지, 라이더-레이더 센서 융합, 사람 특성 곡선, 가려진 물체 감지, 폐색 깊이 생성